

University of New Mexico

## UNM Digital Repository

---

Civil Engineering ETDs

Engineering ETDs

---

Spring 5-15-2021

# EXPLORING THE RELATIONSHIP BETWEEN VEHICULAR EMISSIONS AND TRAFFIC OPERATIONS AT ISOLATED SIGNALIZED INTERSECTIONS

Abiral Dulal  
*University of New Mexico*

Follow this and additional works at: [https://digitalrepository.unm.edu/ce\\_etds](https://digitalrepository.unm.edu/ce_etds)



Part of the [Civil and Environmental Engineering Commons](#)

---

### Recommended Citation

Dulal, Abiral. "EXPLORING THE RELATIONSHIP BETWEEN VEHICULAR EMISSIONS AND TRAFFIC OPERATIONS AT ISOLATED SIGNALIZED INTERSECTIONS." (2021). [https://digitalrepository.unm.edu/ce\\_etds/284](https://digitalrepository.unm.edu/ce_etds/284)

This Thesis is brought to you for free and open access by the Engineering ETDs at UNM Digital Repository. It has been accepted for inclusion in Civil Engineering ETDs by an authorized administrator of UNM Digital Repository. For more information, please contact [disc@unm.edu](mailto:disc@unm.edu).

Abiral Dulal  
*Candidate*

Department of Civil Engineering  
*Department*

This thesis is approved, and it is acceptable in quality and form for publication:

*Approved by the Thesis Committee:*

Assistant Professor Haobing Liu , Chairperson

Assistant Professor Nicholas Ferenchak

Claude Morelli (Research Scholar)

\_\_\_\_\_

\_\_\_\_\_

\_\_\_\_\_

\_\_\_\_\_

\_\_\_\_\_

\_\_\_\_\_

**EXPLORING THE RELATIONSHIP BETWEEN VEHICULAR  
EMISSIONS AND TRAFFIC OPERATIONS AT  
ISOLATED SIGNALIZED INTERSECTIONS**

**by**

**ABIRAL DULAL**

**BACHELOR OF ENGINEERING  
IN  
CIVIL ENGINEERING**

**THESIS**

Submitted in Partial Fulfillment of the  
Requirements for the Degree of

**Master of Science  
In Civil Engineering**

The University of New Mexico  
Albuquerque, New Mexico

**May 2021**

Exploring the relationship between vehicular emissions and traffic operations at isolated  
signalized intersections

Abiral Dulal

Bachelor of Engineering in Civil Engineering

Master of Science in Civil Engineering

## ABSTRACT

Most roadway transportation modes still run on petroleum fuels. Petroleum fuels are major sources of air pollutants, including hydrocarbons (HC), carbon monoxide (CO), carbon dioxide (CO<sub>2</sub>), nitrogen oxides (NO and NO<sub>2</sub>, which are together called NO<sub>x</sub>), Volatile Organic Compounds (VOCs), and particulate matter of size <10 microns (PM<sub>10</sub>) and <2.5 microns (PM<sub>2.5</sub>) including black carbon (BC). These pollutants degrade air quality, have severe effects on public health, and contribute to anthropogenic climate change in some cases (pollutants such as CO<sub>2</sub> and BC). Mitigating pollution is a serious issue, and therefore, it is the engineers' and planners' responsibility to study and reduce emissions as much as possible. Emission levels are generally high at street intersections, which are places where vehicles tend to accelerate, decelerate, and idle. Emission levels at intersections are a function of many different variables, including traffic signal timing and the mix of vehicle types.

This thesis explores how energy consumption levels, emission rates, and emission levels of five pollutants (HC, CO, NO<sub>x</sub>, CO<sub>2</sub>, and PM<sub>2.5</sub>) vary with cycle length, operating modes, and vehicle types at an isolated, two-phase signalized intersection. This study is

based on VISSIM micro-simulation, MOVES emission models, and linear regression analysis (with emission rates as a dependent variable and cycle lengths, delays, and stopping rates as independent variables). A hypothetical intersection is chosen such that the vehicle distribution cars 90%, bus 5% and trucks 5%. The traffic volume is chosen such that V/C ratio is greater than 1. Therefore, a high emission is expected in the intersection and the intersection is reasonable to be optimized for the emission.

A key finding is there is a different optimal range of cycle length for each pollutant: 70s-110s, 100s-120s, 70s-120, 70s -120s, and 60s - 120s for HC, CO, NO<sub>x</sub>, CO<sub>2</sub>, and PM<sub>2.5</sub>, respectively. One of the reasons for different optimal ranges of cycle length for each pollutant is that different vehicle types use different fuel types, with each fuel having a different emission rate for each pollutant. The study also found that even though the proportion of the time travelled by vehicle while accelerating is less, it contributes to the highest proportion of total emissions than travelling in any other operating modes (cruise, decelerating and idle). Therefore, controlling the proportion of travel time in acceleration could help in controlling the amount of emission. The final optimal range of cycle lengths is chosen based on different scenarios. For an intersection in area with a lot of bus services and pedestrians/bikes, like downtown, the optimal cycle range is found to be 70s to 90s. Similarly, for an intersection in area with a large number of trucks and no bikes/pedestrians, like an industrial area, the optimal cycle length is found to be 90s to 110s. And for intersection in suburbs, where there are only cars and no (or few) bikes/pedestrians, buses, and trucks the optima range of cycle length is found to be 80s to 100s.

Finally, the linear regression analysis showed the emission rate of pollutants is negatively correlated with the cycle length and positively correlated with average delay and stopping; however, adding stopping rates as additional independent variables does not significantly improve the model and the correlation is only significant in case of CO and CO<sub>2</sub> even though the relationship is statistically significant for all pollutants.

## Table of Contents

<i>ABSTRACT</i> .....	<i>iii</i>
<i>List of Figures</i> .....	<i>viii</i>
<i>List of Tables</i> .....	<i>ix</i>
<i>Abbreviations</i> .....	<i>x</i>
<b>1 Introduction</b> .....	<b>1</b>
<b>2 Literature Review</b> .....	<b>4</b>
<b>2.1 Traffic operations</b> .....	<b>4</b>
<b>2.2 Energy and emission</b> .....	<b>8</b>
2.2.1 Fuel and Energy in vehicles.....	9
2.2.2 Air quality and emissions in vehicles .....	11
2.2.3 Emission rates and Units.....	12
2.2.4 EPA MOVES and Pollutants .....	12
<b>2.3 Studies on Emission Analysis and Operations at an isolated signalized intersection</b> .....	<b>13</b>
<b>3 Methodology</b> .....	<b>20</b>
<b>3.1 Traffic Signal Design</b> .....	<b>21</b>
<b>3.2 Simulation</b> .....	<b>23</b>
<b>3.3 Data compilation:</b> .....	<b>25</b>
<b>4 Results and Discussion</b> .....	<b>29</b>
<b>4.1 Cycle Length, Delay and Stopping rate</b> .....	<b>29</b>
<b>4.2 Emission and Cycle Length</b> .....	<b>32</b>
<b>4.3 Variation of Emission Rate by Vehicle Type with Cycle Length</b> .....	<b>39</b>
<b>4.4 Variation of Proportion of Operation with Cycle Length</b> .....	<b>41</b>
<b>4.5 Proportion of the vehicle Operations and proportion of the Emissions</b> .....	<b>44</b>
<b>4.6 Proportion of Vehicles and Proportion of Emission</b> .....	<b>50</b>
<b>4.7 Regression Analysis</b> .....	<b>51</b>
4.7.1 Regression between HC emission rate and Cycle length, average delay and average stop.....	51

4.7.2	Regression between CO emission rate and Cycle length, average delay and average stop.....	52
4.7.3	Regression between NOx emission rate and Cycle length, average delay and average stop .....	53
4.7.4	Regression between Energy Consumption rate and Cycle length, average delay and average stop .....	54
4.7.5	Regression between CO <sub>2</sub> emission rate and Cycle length, average delay and average stop .....	55
4.7.6	Regression between PM2.5 emission rate and Cycle length, average delay and average stop .....	56
<b>5</b>	<b><i>Conclusion</i></b> .....	<b>58</b>
<b>6</b>	<b><i>References</i></b> .....	<b>63</b>
	<b><i>Appendix 1: Signal Timing Design</i></b> .....	<b>66</b>
	<b><i>Appendix 2: MOVES Vehicle Type and Physics Parameters</i></b> .....	<b>67</b>
	<b><i>Appendix 3: MOVES VSP/STP Operating Mode Bins</i></b> .....	<b>68</b>
	<b><i>Appendix 4: Age Distribution for year 2020</i></b> .....	<b>70</b>

## List of Figures

Fig: 1: Total share of energy used for Transportation .....	9
Fig: 2 U.S. transportation energy sources/fuels.....	10
Fig: 3 Energy densities of alternative fuels. Source: Davis, Diegal, and Boundy.....	11
Fig: 4: Intersection under study and Traffic Volume .....	20
Fig: 5 Phase for signal timing.....	21
Fig: 6 Average Delay in secs/veh and the Cycle Length.....	30
Fig: 7 Average stop rate in numbers/veh Vs Cycle Length.....	31
Fig: 8 Plot showing the HC emission in gram/veh-mile in each Cycle Lengths in seconds .....	32
Fig: 9 Plot showing the CO emission in gram/veh-mile and Cycle Lengths in seconds.....	33
Fig: 10 Plot showing the NOx Emission in gram/vehicle-mile and Cycle Lengths in seconds.....	34
Fig: 11: Plot showing Energy consumption in KJ/veh-mile and Cycle Length in seconds .....	35
Fig: 12 Plot showing CO <sub>2</sub> in grams/veh-mile and Cycle Length in second.....	36
Fig: 13 Plot showing the PM <sub>2.5</sub> emission rate in grams/veh-mile and Cycle Lengths in seconds.....	37
Fig: 14: Emission rate at different cycle length for different vehicle type for HC, CO, and NOx .....	39
Fig: 15 Emission rate at different cycle length for different vehicle type for energy consumption, CO <sub>2</sub> and PM <sub>2.5</sub> .....	40
Fig: 16 Variation of Proportion of Operations with Cycle Length.....	43
Fig: 17 Proportion of HC Emission by travel time in operation at different Cycle Length .....	44
Fig: 18 Proportion of CO Emission by Operation at different Cycle Length.....	45
Fig: 19 Proportion of NOx Emission by Operation at different Cycle Length .....	45
Fig: 20 Proportion of Energy Consumption by Operation at different Cycle Length .....	46
Fig: 21 Proportion of CO <sub>2</sub> Emission by Operation at different Cycle Length .....	46
Fig: 22 Proportion of PM <sub>2.5</sub> Emission by Operation at different Cycle Length .....	47
Fig: 23: Proportion of operating modes and Emissions .....	49
Fig: 24 Proportions of vehicles and emissions .....	50
Fig: 25 Plot for HC with Cycle Length, Average delay, and Average stop .....	51
Fig: 26: Result of Regression for Pollutant 1(HC) .....	52
Fig: 27 Plot for CO with Cycle Length, Average delay, and Average stop .....	52
Fig: 28 Result of Regression for Pollutant 2 (CO) .....	53
Fig: 29 Plot for NOx with Cycle Length, Average delay, and Average stop .....	53
Fig: 30 Result of Regression for Pollutant 3 (NOx) .....	54
Fig: 31 Plot for Energy with Cycle Length, Average delay, and Average stop .....	54
Fig: 32 Result of Regression for Pollutant 3 (Energy) .....	55
Fig: 33 Plot for CO <sub>2</sub> emission with Cycle Length, Average delay, and Average stop .....	55
Fig: 34 Result of Regression for Pollutant 98 (CO <sub>2</sub> ).....	56
Fig: 35 Plot for PM <sub>2.5</sub> emission with Cycle Length, Average delay, and Average stop.....	56
Fig: 36 Result of Regression for Pollutant 110 (PM <sub>2.5</sub> ).....	57

## List of Tables

Table 1: Signal Green Time and Intersection V/C ratio .....	23
Table 2: Vehicle types and fuel types.....	27
Table 3: Minimum emission of Pollutants and Cycle Length .....	38
Table 4: The categories of the vehicle operation mode.....	42
Table 5: Proportions of operating modes at webster's optimal cycle length and optimal cycle length for emission.....	48

## Abbreviations

CO	: Carbon monoxide
CO <sub>2</sub>	: Carbon dioxide
NO <sub>x</sub>	: Nitrogen Oxide
HC	: Hydrocarbon
PM	: Particulate Matter
VOCs	: Volatile Organic Compounds
GHGs	: Green House Gases
EPA	: Environmental Protection Agency
MOVES	: Motor Vehicle Emission Simulator
VSP	: Vehicle Specific Power
EFs	: Emission Factors
STP	: Scaled Tractive Power
BTU	: British Thermal Unit
gm	: gram
veh-mile	: vehicle-mile
KJ/s	: Kilo Joule per second
J	: Joules
F	: Fahrenheit
CMEM	: Comprehensive Modal Emission Model
VISGAOST	: Vissim-based genetic algorithm optimization of signal timings
Vph	: Vehicle per hour

## 1 Introduction

While there have been many recent advances in vehicle electrification and other advanced technologies, most transportation modes continue to rely on energy derived from fossil fuels. Fossil fuels have several advantages over other fuel sources, including high availability compared to annual use, high energy density, ease of storage, ease of transportation, etc. Because most transportation modes run on fossil fuels, they emit pollutants like Carbon monoxide (CO), Carbon dioxide (CO<sub>2</sub>), Nitrogen Oxide (NO<sub>x</sub>), particulate matter, Volatile Organic Compounds (VOCs), etc. These pollutants deteriorate the air quality, which is one of the factors that affect the quality of life of people because it has a direct impact on public health. According to the United States Environmental Protection Agency, “the transportation sector is one of the largest contributors to anthropogenic U.S. greenhouse gas (GHG) emissions. According to the Inventory of U.S. Greenhouse Gas Emissions and Sinks 1990-2018 (the national inventory that the U.S. prepares annually under the United Nations Framework Convention on Climate Change), transportation accounted for the largest portion (28%) of the total U.S. GHG emissions in 2018. Cars, trucks, commercial aircraft, and railroads, among other sources, all contribute to transportation end-use sector emissions” (EPA, 2020).

Air quality has a significant impact on people’s health, and air pollution has severe health risks. The impact of poor air quality ranges from increased risk of respiratory diseases to cancer. According to one of the reports of the Union of Concerned Scientists, “nearly one-half of everyone living in the United States (an estimated 150 million people) live in areas that do not meet federal air quality standards. The passenger cars and heavy-duty trucks

are major sources of this pollution” (UCS, 2014). Therefore, transportation professionals should be aware of this when planning and designing transportation systems.

Transportation engineering deals with planning, design, operation, and maintenance of safe and efficient transportation systems, i.e., to develop a sustainable transportation system. The system should be developed to have less impact on public health as far as possible to develop a sustainable transportation system. Therefore, engineers must model the transportation system so that the emission of pollutants should be less in the total life cycle of the transportation system. One of the important areas in the transportation system’s life cycle where engineers need to intervene is to reduce the emission during traffic operations to improve air quality.

“Traffic operations deal with the planning for and controlling the movements of vehicles and groups of vehicles over the street and highways for the purpose of attaining maximum efficiency and safety” (Marsh, 1949). While obtaining maximum efficiency and safety, it is also essential to optimize the traffic operations parameters such as cycle length, delay and stopping rates, etc., at an intersection for emission reduction because the emission depends upon these parameters and is high at an intersection. Furthermore, accelerations and decelerations, operations associated with high emission, occur more at signalized intersections. Moreover, “many past studies have reported on the variation of emission factors with average vehicle speed; the largest Emission Factors (EFs) for CO and other pollutants tend to occur at speeds of less than 20 mph because of inefficient engine operation primarily due to stop/ start an activity and frequent idling/acceleration” (Abou-

Senna, Radwin, KurtWesterlund, & Cooper, 2013). This thesis attempts to explore the relationships between emissions and the traffic operations parameters of the intersection such as traffic signal cycle lengths, delays, stop frequencies, operating modes, etc., so that the intersection could be optimized for less emission.

According to Karen R. Den Braven (2012), Environment Protection Agency (EPA) 's emission and fuel consumption data can be combined in several ways with micro-simulation tools like VISSIM (Braven, Abdel-Rahim, Henrickson, & Battles, 2012). In this thesis, it is done using the MOVES-matrix. In the MOVES- matrix, the detailed emissions and fuel consumption data from EPA's can be matched with the operating BinID (a function of speed, acceleration, and VSP) computed from Vehicle Specific Power (VSP) speed and acceleration.

In this thesis, VISSIM is used to model the micro-simulation to obtain the second-by-second result of speed, acceleration, delay, stopping frequencies, etc., which can be used in MOVES-matrix for the analysis.

## 2 Literature Review

### 2.1 Traffic operations

#### a. Headways

The queue is a line of vehicles that stops during the red-light. When the signal turns green line, the vehicle starts moving from the stop. The 1<sup>st</sup> headway is the time lapse between the initiation of Green Signal and the time the front wheels of the first vehicle cross the stop bar. The 2<sup>nd</sup> headway is the time-lapse from the first vehicle's front wheels cross the stop bar until the second vehicles front wheel crosses the stop bar. Subsequent headways are similarly measured. HCM defines start-up lost time as the additional time, in seconds, consumed by the first few vehicles in a queue at a signalized intersection above and beyond the saturation headway due to the need to react to the imitation of the green phase and to accelerate to a steady flow condition.

#### b. Saturation Flow

After some time of initiation of the green phase, the traffic attains constant headway. The flow after that is Saturation flow. HCM recommends using the 5<sup>th</sup> vehicle following the beginning of green as the starting point of the saturation flow rate. The maximum hourly volume that can pass through an intersection from a given lane or group of lanes if that lane (or lanes) were allocated constant green over the course of an hour is called saturation flow rate and is given by

$$S_0 = \frac{3600 \text{ sec}}{h}$$

Where:

$h =$  constant headway (sec/veh)

$S_0 =$  saturation flow rate (typically 1900 passenger car/hour/lane corr. to  $h \sim 1.9$ )

The saturation flow rate can be adjusted using different adjustment factors

c. Lost time:

The portion of a cycle that is not utilized by traffic due to continuous alternating of the right of way between conflicting movements is called lost time. It is the sum of Start-up lost time and Clearance lost time

i. Start-up lost time ( $t_{st}$ ):

It occurs when the signal turns from red to green. The vehicle in the queue does not instantly start moving at the saturation flow rate; there is an initial lag due to driver reacting to the signal change. This lag is called Start-up loss time.

ii. Clearance lost time ( $t_{cl}$ ):

It occurs when the signal turns from green to yellow and a later portion of the yellow and all red is generally not used by the traffic.

d. Effective Green:

It is the time during a cycle that is utilized by traffic for the movement in the intersection and given by

$$g = G + Y + RC - t_L$$

Where:

$g =$  *effective green time in sec,*

$G =$  *actual green interval,*

$RC =$  *actual Red Clearance Interval,*

$t_L =$  *total lost time for the movement during the interval*

Effective Red:

It is the time during a cycle that is not utilized by the traffic for the movement in the intersection and is given by

$$r = R + t_L$$

Where:

$r =$  *effective red time in sec*

$R =$  *time within a cycle for which a movement or combination of movements receives a red indication (RC excluded, sec)*

$t_L =$  *total lost time*

e. Capacity:

The maximum sustainable hourly flow rate at which persons or vehicles can be reasonably expected to traverse a point or uniform section of a lane or roadway during a given time-period under prevailing traffic conditions.

f. Capacity at the Intersection Approach:

Hourly volume which can be accommodated on an intersection approach given that the approach will receive less than 100% (i.e., 3600 seconds) of green time.

$$c = s \left( \frac{g}{C} \right)$$

Where:

$c$  = capacity at intersection approach(veh/hr/lane)

$s$  = saturation flow rate(veh/hr/lane)

$g$  = effective green (sec)

$C$  = cycle length (sec)

g. Cycle length:

The minimum cycle length is given by:

$$C_{min} = \frac{L \times X_c}{X_c - \sum_1^n \left( \frac{CLV}{s} \right)_i}$$

Where:

$C_{min}$  = minimum Cycle length

$L$  = total Lost time in seconds

$X_c$  = Critical V/C ration for the intersection

$CLV$  = Critical Lane Volume

$s$  = Saturation flow rate

The Optimal Cycle length is given by Webster formula as:

$$C_{opt} = \frac{1.5L + 5}{1 - \sum_1^n \left( \frac{CLV}{s} \right)}$$

Where:

$C_{opt}$  = Optimal Cycle length

h. Delays

Control Delay

The component delay that results when a control signal causes a lane group to reduce speed or stop. It is measured by comparison with the uncontrolled condition. Control delay is the service measure that defines the LOS of an intersection. One of the purposes of the signal design is to minimize control delay. The delay types are described below:

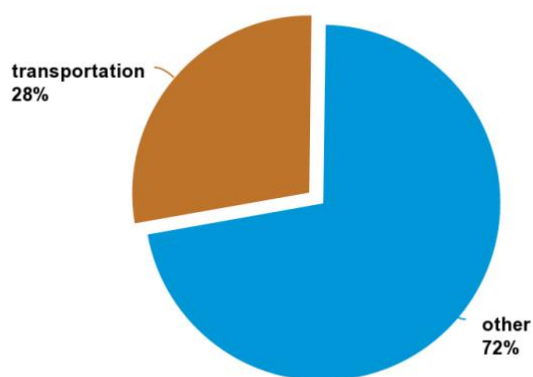
- i. Stopped-time delay: the time a vehicle is stopped in a queue while waiting to pass through the intersection
- ii. Approach delay: includes stopped-time delay but adds the time loss due to deceleration from the approach speed to a stop and the time loss due to reacceleration back to the normal speed
- iii. Travel time delay: the difference between the driver's expected travel time through the intersection and actual time taken

## 2.2 Energy and emission

The transportation sector is one of the major consumers of energy. According to the US Energy Information Administration (EIA), in 2019, after the industry sector (32%), transportation is the second-highest consumer of energy (28%). Unlike in the 1800s, when only a handful of wealthy elites could afford to travel in mechanized vehicles, now millions

of the people in industrial countries have access to mechanized transportation. (Vanek, Angenent, Banks, Daziano, & Turnquist, 2014). Moreover, according to Vanek et al., a large number of upper- and middle-class people expect to travel in their private car; therefore, the large energy consumption in the transportation sector is inevitable on a per-person basis. Furthermore, they also require a large volume of freight all around the world as products from all over the world are transported to any country in the world, even to the consumer's doorsteps. All of these made the transportation sector one of the major energy consumers in the world. Similarly, transportation is also one of the sectors primarily responsible for the large amount of GHGs emissions and pollutants NO<sub>x</sub>, particulate matter, and VOCs.

**Share of total U.S. energy used for transportation, 2019**



 Source: U.S. Energy Information Administration, *Monthly Energy Review*, Table 2.1, May 2020, preliminary data

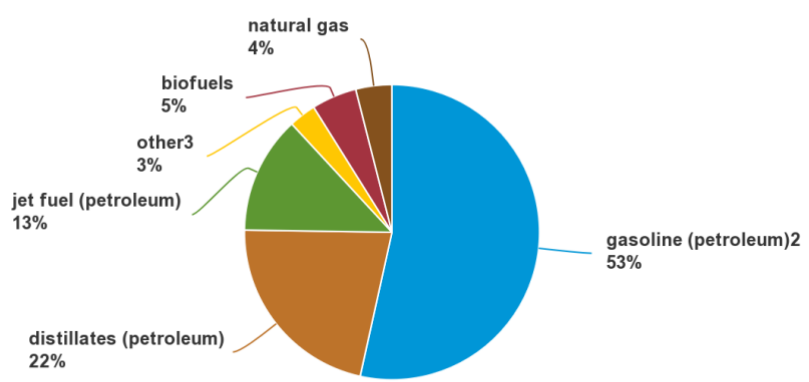
Fig: 1: Total share of energy used for Transportation

### 2.2.1 Fuel and Energy in vehicles

In the transportation sector, petroleum is the most dominant energy source. According to the US Energy Information Administration, 2019, 88% of the energy is derived from

petroleum (incl. gasoline (53%), distillates (22%) and jet fuel (13%). Other 12% is total of biofuel (5%), natural gas (4%), and others (3%). The dominance of petroleum is because it has several advantages over alternative transportation fuels. One of the reasons is the world's petroleum resource is large compared to the annual petroleum use (Giuliano & Hanson, 2017). Another advantage is that petroleum fuels have high energy density than other alternative fuels. Similarly, the transportation of petroleum fuels is relatively easy.

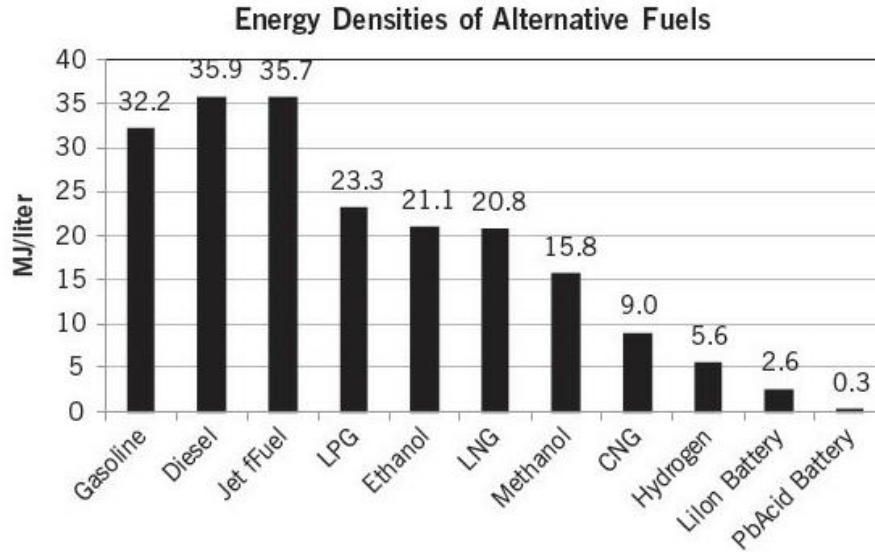
U.S. transportation energy sources/fuels, 2019 1



1. Based on energy content  
2. Motor gasoline and aviation gas; excludes ethanol  
3. Includes residual fuel oil, lubricants, hydrocarbon gas liquids (mostly propane), and electricity (includes electrical system energy losses).  
Note: Sum of individual components may not equal 100% because of independent rounding.  
Source: U.S. Energy Information Administration, *Monthly Energy Review*, Tables 2.5, 3.8c, and 10.2b, May 2020, preliminary data



Fig: 2 U.S. transportation energy sources/fuels



Gaseous fuels are assumed to be stored under pressure: CNG at 25 MPa, hydrogen at 70 MPa.

Fig: 3 Energy densities of alternative fuels. Source: Davis, Diegal, and Boundy

### 2.2.2 Air quality and emissions in vehicles

According to the definition of EPA, "Emissions" is the term used to describe the gases and particles put into the air or emitted by various sources. The amount of each type of emissions changes from year to year and is caused by the change in the economy, technology, industrial activities, and other factors. The change in the policy and air quality regulations also significantly affect the change in the quantity of emissions. There are different programs and standards in the US to reduce smog and other air pollutants from transportation, such as Passenger Vehicle Standard, Heavy Duty Diesel Engine Standards, National Clean Diesel Standards, Smart way for Freight standards, etc.

The principal emissions from the automobile are CO, HC, GHGs (99% of CO<sub>2</sub>), NO<sub>x</sub>, Particulate Matters, and VOCs. Green House Gases (GHGs) are emitted from the tailpipe of automobiles and that combusted fuels and stays in the atmosphere for over 100 years

and more. Moreover, GHGs traps the energy in the atmosphere and act like a blanket around earth, causing it to warm and rise in temperature. This can lead to change in earth's climate and raise sea levels. It also results in severe effect on human health and welfare and to ecosystems. Automobiles combusting fuels also emit CO, HC, NO<sub>x</sub>, VOCs, Particulate Matters, which forms smog. The smog is trapped near the ground level, forming a haze that pollutes the air. Smog can significantly affect the health of the people causing difficulty in breathing and triggering lung diseases such as asthma, emphysema, etc., which may cause untimely death. (EPA, 2019)

### 2.2.3 Emission rates and Units.

The transportation system uses large quantities of energy and therefore, the energy is measured in terms of exajoules(1EJ=10<sup>18</sup>joules) or quad BTU. A joule is defined as the work done by applying a force that can accelerate 1 kilogram by 1 meter per second squared over the distance of 1 meter. A Btu is the amount of energy required to raise the temperature of 1 pound of water by 1°F. One Btu equals 1,055 joules.

The rate of emission from a vehicle is measured in gm/s. The rate of emission for vehicles traveling in a roadway is measured in gm/vehicle-mile. The energy generated from combusted in the vehicle is measured in KJ/s.

### 2.2.4 EPA MOVES and Pollutants

EPA's Motor Vehicle Emission Simulator (MOVES) is an emission modeling system that incorporates speed, acceleration, vehicle specific power, and vehicle model year to

estimate the emission rate of different pollutants from a mobile source. The MOVES-matrix is a simplified version of MOVES that can be used to do similar modeling.

There are various codes for these pollutants, and these pollutants are given a code number. The ones used in the analysis are listed below.

There are various codes for these pollutants, and these pollutants are given a code number.

The ones used in the analysis are listed below.

Pollutant 1 = Hydrocarbon (HC)

Pollutant 2 = Carbon monoxide (CO)

Pollutant 3 = Nitrogen Oxide (NO<sub>x</sub>)

Pollutant 91= Energy Consumption

Pollutant 98= Carbon dioxide (CO<sub>2</sub>)

Pollutant 110 = 2.5-micron Particulate Matter (PM<sub>2.5</sub>)

### 2.3 Studies on Emission Analysis and Operations at an isolated signalized intersection

When a vehicle approaches a red light at an intersection, it first decelerates and then comes to a complete stop in an unsaturated condition. It stops for some time until the green light is on. Then it starts to accelerate when the green light is on. A typical vehicle operating mode consists of deceleration, stop (idle), acceleration, and cruise (vehicle move at constant speed). “Vehicles decelerating, stopping, and accelerating near the intersections of urban streets result in high levels of emissions” (Li, Wu, & Zou, 2011). These operations are associated with delay, stoppings, and emissions.

Li et al. (2004) proposed a signal timing model to optimize cycle length and green time to reduce emissions at intersections. The model is based on the performance index. The case study was done in one of the intersections located in Nanjing City. The study concluded that when signal cycle length increases, there is an optimal value corresponding to performance index, which optimizes delay, fuel consumption, and emission at the intersection (Li, Li, Pang, Yang, & Tiang, 2004).

Wang et al. (2009) conducted a study to optimize the signal time based on vehicle emission. The team examined the amount of emission that could be reasonably reduced by changing the signal timing program. Green timing was changed in this study. The study was done for the Changchun city in China. The paper showed that a change in signal timing program could reduce emission and delay time at the intersection. (Wang, Guo, Shiwu Li, Wang, & Li, 2009)

Li et al. investigated the impact of the signal timing on vehicle emission at an intersection with pre-timed signalization. It was carried in two steps: first, vehicle micro-simulation was carried out to model vehicle trajectories, and second, models are used to determine the emission. This study's first primary process was to examine the trade-off between vehicle delays and the number of stops. The second step is to estimate the emission based on the outcome of the first process. In this study, only VSP is used to estimate the emission. The research concluded that "reducing emissions is not simply equivalent to reducing the number of stops because delays and stops are correlated in urban traffic" (Li, Wu, & Zou,

2011). Also, it was concluded that reducing stops may result in reducing the CO emission, but the amount of CO<sub>2</sub> was slightly increased, and there was no significant effect on HC and NO<sub>x</sub>

Another attempt was made by Wu et al. (2020) to optimize Urban traffic signal timing by reducing vehicle emission. The optimization is done in the green light duration keeping the phase design and the cycle length the same as that of the original signal timing scheme. A new model was used to calculate the emission, and a genetic algorithm was used for optimization. The MOVES model was not used to estimate emission because of the wide input parameter. The study found that the signal control optimization model effectively reduced the emission in one of the intersection groups in Kunshan city (Wu, Sun, & Liu, 2020)

Chen & Yu (2007) developed the integrated microscopic traffic-emission simulation platform for evaluating the Traffic Control strategies. They used VISSIM for micro-simulation and CMEM (Comprehensive Modal Emission Model) for determining the emission. This research analyzes the relationship between the instantaneous emission /fuel consumption rate and the instantaneous speed/acceleration. According to Chen & Yu, many statistical methods have been used by various researchers to quantify the traffic emissions; however, they found that they are not accurate because they cannot capture the dynamic traffic flow scenarios. Therefore, a micro-simulation model like “VISSIM is necessary, a microscopic, time step and behavior-based simulation model that can be used to model traffic operations in the urban road network and highway corridors, the transit

and mixed traffic operations” (Chen & Yu, 2007). Chen et al. also stated that VISSIM uses the psycho-physical driver behavior model developed by WIEDEMANN (1974) compared to the less complex model using constant speed and deterministic car following logic. In this study, they found that emission increase with the increase in vehicle speed and acceleration; especially when there is acceleration, the instantaneous emission increases sharply. The research also showed that when the instantaneous acceleration is unchanged and negative, the emission and fuel consumption increase slowly as the vehicle’s speed increases. The research concluded that the emission from vehicles is dependent on the vehicles’ operating modes (Chen & Yu, 2007).

Stevanovic et al. (2009) put forward an approach to optimize traffic control to reduce fuel consumption and Vehicular Emission. To optimize the traffic control, they linked VISSIM, CMEM, and VISGAOST. However, they concluded the fuel consumptions are inadequately estimated by the formula commonly used to estimate the fuel consumption in the traffic simulation tools and, therefore, cannot be used in traffic signal optimization (Stevanovic, Stevanovic, Zhang, & Batterman, 2009).

Rao et al. (2014) analyzed the instantaneous vehicle emission models based on speed and acceleration. In this study, the relationship between speed/acceleration and emission is analyzed qualitatively and quantitatively, and finally, the emission model was established. Real-world data were used in the analysis. The research found that the emission rate is lowest at idle, and with the increase in speed, the emission also increased; however, when the speed reached a specific value, the engine speed increased too, the combustion is full,

and the emission is reduced. This effect is shown by HC, NO<sub>x</sub> with relatively small change. However, the CO decline rapidly. The study also showed that the NO<sub>x</sub> is decline with an increase in acceleration and the emission of CO and HC changed relatively with a change in acceleration. Finally, the results of the instantaneous speed/acceleration models were compared with CHEM based on VISSIM, and they showed satisfactory results (Rao, Zhang, Yang, & Fang, 2014).

LeBlanc et al. studied the impact of the driving pattern variability on Carbon Monoxide emission. The authors suggest that the emission from the vehicle is dependent on the vehicle type and vehicle activity. It is also dependent upon the transportation network characteristics and driver characteristics. According to the study, operating modes characteristics such as accelerating rates cruise speed distribution rates are necessary while developing an emission model. The reason is that particular vehicle and engine operating modes are the sources of high emission rates. The research also suggests that the emission model developed for CO in this study is not applicable in the case of HC, NO<sub>x</sub>, and other pollutants because they behave differently. The model developed is used to estimate the relative CO emissions associated with the differences in operating profiles. The study concluded that the models based only on speed and acceleration profiles might not be adequate to estimate CO emission rate because the study showed large variability in response to change in operating modes vehicle-to-vehicle. The study recommends integrating driving behavior and pattern (a function of infrastructure, fleet characteristics, and demographics) (LeBlanc, Saunders, Mayers, & Guensler, 1995).

Frey et al. (2000) evaluated the effect of traffic signal coordination and timing on real world emission. Tail-pipe emission was measured on-road second-by-second. The study concluded the traffic signal could have a significant impact on emission. Based on the on-road data, the study found that the average emission rate during acceleration is substantially higher than in deceleration, cruise, and idle, which is different from the conventional assumption that the emission during idle is greater than when the vehicle is moving. Furthermore, the peak in the emission is strongly connected with the accelerations. The study also suggests that acceleration is are strongly influenced by signalization.

Many attempts have been made to study the relationship between emissions and different operations. Some studies have proposed some complicated algorithms like genetic algorithms, while others have attempted using performance indices. However, it is necessary to see the effect of vehicle distribution and the proportion of time for each operating mode (acceleration, cruise, deceleration) that could impact different emission types. These studies have not attempted to study the emission by breaking the study by vehicle type and operation modes. Furthermore, most of these studies have fixed cycle length and have tried to optimize the green time and do not study emission reduction when the cycle length is changed.

Similarly, the cycle length also impacts the intersection V/C ratio, which controls the delay's nature if it is excess or unstable or not significant and thus affects the vehicle's emission. Moreover, the cycle length also controls the vehicle travel time proportion in different operation modes on which the emission rates depend. Therefore, there is a need

to study the effect on emission rate due to each vehicle type at different cycle lengths and each operating mode.

In this thesis, the study is done for three vehicle types: cars, buses, and trucks, with the vehicle distribution 90%, 5%, and 5%, respectively. The emission rate for car, bus, and trucks are estimated in grams/veh-mile and compared. Similarly, the proportion of each vehicle type is compared with the proportion of emissions due to each vehicle type. Also, the proportion of the time the vehicle travels in a specific operation mode is compared with the emission proportion during each operating mode. This is to know the extent of the effect of each operating mode on the emission rates.

### 3 Methodology

A simple four-legged intersection with two-way movement is chosen for the study, having only through movements and no left turns or right turns. The intersection has one major road (EW) and other minor roadways (NS). A hypothetical traffic volume data of 2400 vph is chosen so that the traffic signal could be designed for it. The intersection capacity suggested by HCM Quick Estimation Method is 1710 vph. For the intersection to have excessive delay and queuing, the intersection traffic volume of 2400 vph is assumed so that the volume-to-capacity ratio is greater than one and the emission characteristics could be studied. The vehicle distribution used for the simulation is cars (90%), buses (5%), and trucks (5%). The reason for selecting this kind of intersection is that this intersection will have high emission, and it is reasonable to optimize signal timing for the emission. The traffic volume is divided as shown in fig: 4 below in such a way that there is a minor and major road.

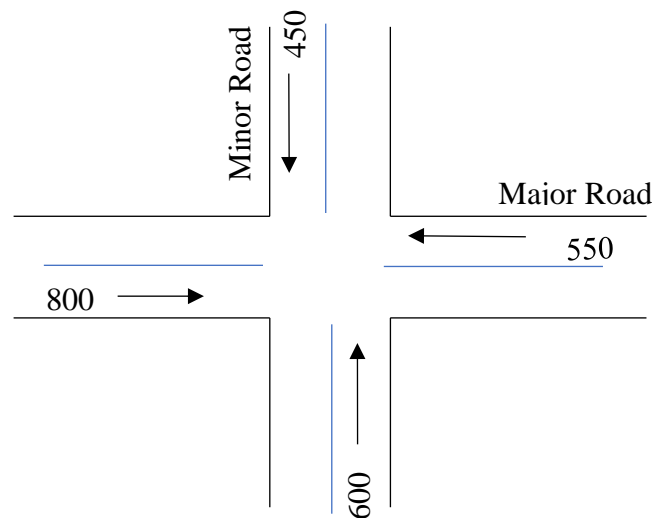


Fig: 4: Intersection under study and Traffic Volume

### 3.1 Traffic Signal Design

The study is done for the different cycle lengths from 20 seconds to 120 seconds at an interval of 10 seconds. The signal timing is designed for all the cycle lengths. The process of signal timing design is listed below:

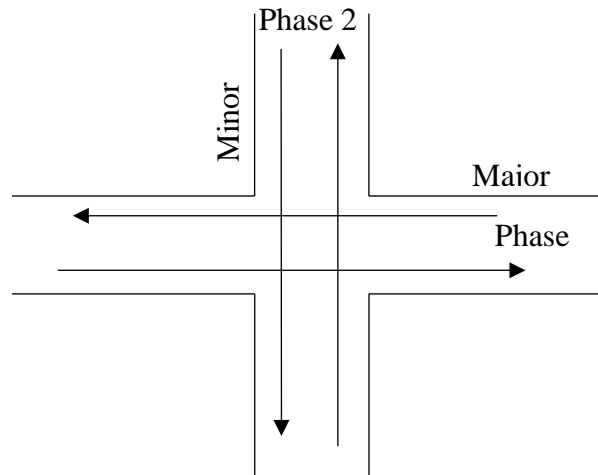


Fig: 5 Phase for signal timing

- A critical lane volume is obtained by comparing the volume in the consecutive movements in phase 1 and then phase 2. Then the critical lane volumes are added to get the critical intersection volume (CS).
- Then reference sum is calculated which is given by

$$RS = 1530 \times PHF \times f_a$$

Where:

$PHF$  = Peak Hour Factor (assumed 1)

$f_a$  = adjustment factor for the area (assumed 1)

- Then the cycle length  $C$  and Lost time  $L$  is assumed. Lost time is assumed 4 seconds for each phase.
- Assess intersection volume to capacity ( $V/C$ ) ratio is calculated as

$$X_{cm} = \frac{CS}{RS \left(1 - \frac{L}{C}\right)}$$

- The critical ratio for phases is

$$y_i = \left(\frac{v}{s}\right)_i^c$$

Where:

$$\left(\frac{v}{s}\right)_i^c = \text{critical volume / saturation rate for phase } i$$

- Then green and yellow time for the phase is calculated as

$$G_i = \frac{y_i}{\sum y_i} (C - L)$$

$$Y_i = T + \frac{S}{2(a + G)}$$

Where:

$T$  = driver reacting time (assumed 1 sec)

$S$  = posted speed (assumed 45 mph)

$a$  = vehicle acceleration (assumed 10 ft/s<sup>2</sup>)

$G$  = approach grade %

- All red is assumed to be 1 second

- Red duration is calculated as

$$R = C - (G_i + Y_i + AR_i)$$

Where:

$C$  = cycle length

$Y_i$  = total Yellow time for the phase  $i$

$AR_i$  = total loss time for the phase  $i$

The calculation for the signal timing is shown in appendix 1. The signal timing is used in the VISSIM for simulation which is summarized below:

Table 1: Signal Green Time and Intersection V/C ratio

SN	Cycle lengths (secs)	Green Time (secs)		Intersection V/C (Remarks)
		Phase I	Phase II	
1	20	10	7	1.53 (Excessive delays and Queueing anticipated)
2	30	15	12	1.25 (Excessive delays and Queueing anticipated)
3	40	21	16	1.14 (Excessive delays and Queueing anticipated)
4	50	27	20	1.09 (Excessive delays and Queueing anticipated)
5	60	32	24	1.06 (Excessive delays and Queueing anticipated)
6	70	38	29	1.03 (Excessive delays and Queueing anticipated)
7	80	44	33	1.02 (Excessive delays and Queueing anticipated)
8	90	50	37	1.00 (Unstable flow results wide range of delay)
9	100	55	42	0.99 (Unstable flow results wide range of delay)
10	110	61	46	0.99 (Unstable flow results wide range of delay)
11	120	67	50	0.98 (Unstable flow results wide range of delay)
12	130	72	54	0.98 (Unstable flow results wide range of delay)
13	140	78	59	0.97 (Unstable flow results wide range of delay)
14	150	84	63	0.97 (Unstable flow results wide range of delay)
15	160	90	67	0.96 (Unstable flow results wide range of delay)

### 3.2 Simulation

The micro-simulation is performed in the VISSIM, “a microscopic, time step and behavior-based simulation model that can be used to model traffic operations in the urban road

network and highway corridors, the transit and mixed traffic operations” (Chen & Yu, 2007). In contrast with other simpler models, the VISSIM incorporates a psycho-physical driver behavior model and can represent accurate real-world conditions.

The simulation parameters used are as follows:

Simulation resolution: 1 Time step(s)/Simulation seconds

Random seeds: 42

Number of simulations runs: 30

Random seed increment: 1

The simulation is done for a base scenario which is optimal cycle length (67 s). The other scenarios were created for cycle length 20s, 30s, 40s, 50s, 60s, 70s, 80s, 90s, 100s, 110s, 120s, 130s, 140s, 150s, and 160s, and simulations were performed. The signal timings for red and green are designed for the traffic flow, as shown in Appendix 1. The vehicle distribution chosen is 90% passenger cars, 5% buses, and 5% trucks.

The micro-simulation in the VISSIM produces the second-by-second value of speed, acceleration, delay, number of stoppings, and number and position of the vehicle for each simulation. The VISSIM model is done as shown in the following steps:

- i. Create a Base Scenario and set up the desired unit
- ii. Build a network
- iii. Input vehicle/ volume data
- iv. Add vehicles and enter vehicle composition
- v. Add signal control
- vi. Add detectors

- vii. Create scenarios with modification in the signal control for all cycle lengths. The data of the signal control is shown in Appendix 1
- viii. Set up for the direct output of simulation seconds, vehicle no, speed, acceleration, delay, stopping distance
- ix. Run the simulation using the parameters above.

For each scenario, the number of simulation runs is 30. The numbers of simulation runs are done to normalize the error/variability in output due to the randomness—the random seed used in 42. The randomness will occur on the vehicle's number in the simulation, speed, acceleration, delay, and stopping. These data are important, and simulation is run 30 times to normalize the variability/error.

### 3.3 Data compilation:

The direct output data from the VISSIM is then compiled. The steps for the compilation for the data is as follows:

- i. The second-by-second output of speed and acceleration is used to calculate the Vehicle Specific Power (VSP: a function of speed & acceleration) and is given by:

$$VSP/STP = \left(\frac{A}{M}\right) v + \left(\frac{B}{M}\right) v^2 + \left(\frac{C}{M}\right) v^3 + \left(\frac{m}{M}\right) (acc + g \times \sin\theta)v$$

Where:

$VSP =$  vehicle specific power (kW/tonne, power to weight ratio)

$STP =$  scaled tractive power (KW/tonne)

$v =$  second-by-second velocity (m/s)

$acc =$  second-by-second acceleration (m/s<sup>2</sup>)

$g =$  gravitational acceleration (9.81 m/s<sup>2</sup>)

$\theta =$  road grade (radians or degrees, as required by the sin calculation algorithm)

$m =$  vehicle mass (tonnes)

$A =$  rolling resistance (KW-s/m)

$B =$  rotating resistance (KW-s<sup>2</sup>/m<sup>2</sup>)

$C =$  aerodynamic drag (KW-sec<sup>3</sup>/m<sup>3</sup>)

$M =$  fixed mass factor for the source type (tonnes)

The table for the for the coefficient for Bus, Car and Truck is shown in the appendix:2

- ii. Then After the calculation of the VSP/STP the vehicle operating mode binID is established for each second based on VSP, speed and acceleration. binID (OpmodeID) is the function of VSP, speed and acceleration. This is called binning approach. There are four types of operations that is defined by binID: braking, idle, coast, and acceleration/cruise. Based on the combination of ranges of acceleration, speed and VSP these modes and Operating mode ID or binID are defined which is shown in Appendix 3.
- iii. After binID (opmodeID) has been established for each second of the operations, the age is assigned to each vehicle randomly in the proportion recommended by the EPA vehicle age distribution. The age distribution for the year 2020 is taken, shown in Appendix 4. The random age distribution is assumed to emulate the real-world scenario for each simulation. In this analysis, the distribution is randomly used in the vehicles running in the intersection. Since 30 simulations are carried out, the age distribution is used randomly for each vehicle in each simulation.

- iv. The fuel type is then assigned by assigning VehicleFuelTypeID based on VehicleTypeID for each vehicle type. The vehicle type and fuel type and their ID is shown in table below:

Table 2: Vehicle types and fuel types

SN	Vehicle Type	VehicleTypeID	Fuel	VehicleFuelTypeID
1	Car	21	Gasoline	1
2	Bus	42	Diesel	2
3	Truck	62	Diesel	2

- v. Now the combination of binID, VehicleTypeID, VehicleFuelTypeID and PollutantID, VehicleModelYearID are matched with the EPA database to get the rate of each pollutant in the emission in grams/seconds (KJ/s for pollutantID 91). This table for each combination is obtained from the EPA's database. Thus, the rate of emission for each pollutant for each second is obtained.
- vi. The compiled data is divided according to different vehicle types for the analysis.
- vii. Further summarization is done for the analysis. The total vehicle-seconds could be obtained by counting each second in the simulation run. The total number of the vehicles is obtained by counting the number of unique vehicle id in the VISSIM output file. The total distance traveled by the vehicle could be obtained by adding the speeds in each second. The average speed could be obtained by dividing the distance by the total simulation second and then converting it into the desired unit. The average delay and stops are obtained by dividing the total delay and stops by the vehicle-seconds or vehicle-mile as required. The average emission in gm/veh-mile for each simulation is obtained by adding the emission rate and dividing my total distance. This is done for all six pollutants

viii. These all data are then compiled into one summary

## 4 Results and Discussion

At first, the trend of delay and stopping rates with the Cycle length was studied. Similarly, the trend of emissions of different pollutants with the cycle length under study according to the vehicle type was also studied. Furthermore, in this thesis, the proportion of the number of each vehicle type (Car, Bus, and Truck) is compared with the quantity of emissions they produce. The proportion of emission is compared with the proportion of the vehicle operating modes such as acceleration, cruise, deceleration, and idle. Similarly, the observations of the trend of the average of each emission rate with the cycle length were also done. Finally, a regression analysis was done between the emissions and cycle length, delay, and stopping rates.

### 4.1 Cycle Length, Delay and Stopping rate.

The second-by-second output from VISSIM gives the cumulative delay and stopping for each vehicle. The output is then compiled to get the average delay and stopping for each cycle length. Each delay is added for each cycle length, and then it is averaged over the veh-mile traveled which can also be obtained from the output from the VISSIM simulation. Then Average delay (in sec/veh-mile) Vs. Cycle length (in seconds) is plotted as shown in fig:6. Similarly, average stopping (in numbers/veh-mile) Vs. Cycle length (in second) is also plotted as shown in fig: 7.

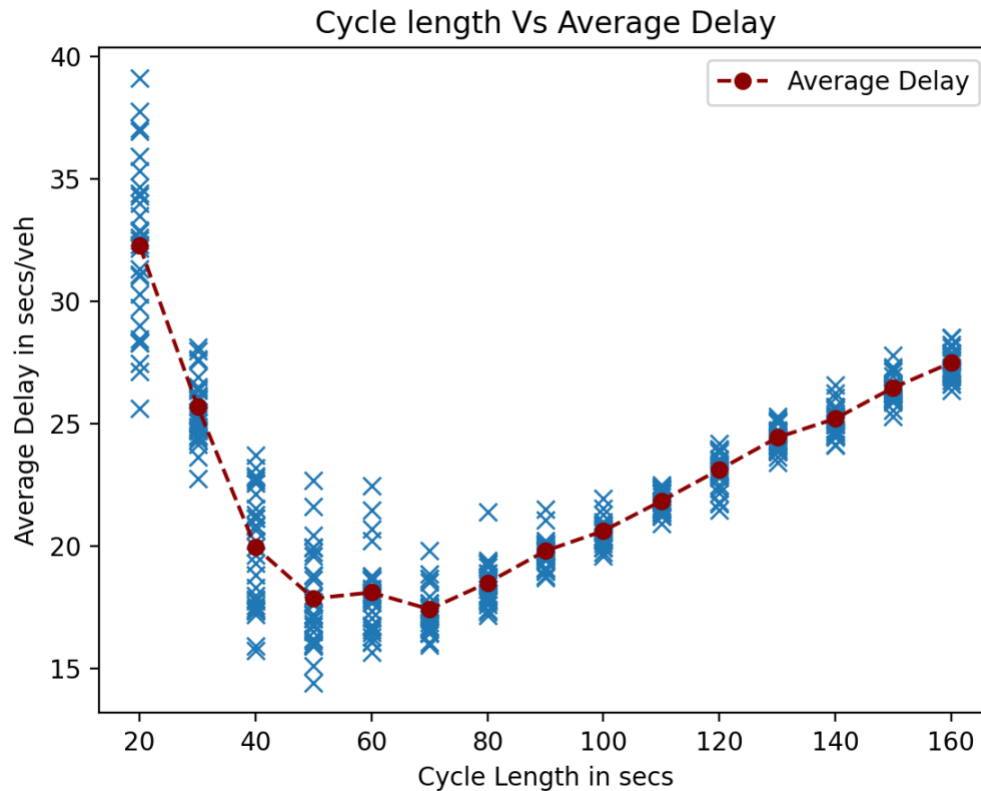


Fig: 6 Average Delay in secs/veh and the Cycle Length

This plot shows that the average delay decreases rapidly from cycle length 20 seconds to 50 seconds when the cycle length is not optimal. After the 50s-70s, the delay starts to increase. Therefore, this graph indicates the optimal cycle length for the minimum delay is around 50-70 seconds. The graph also supports the fact that signal timing is designed to reduce the delay. The optimal cycle length given by the Webster's formula is around 67 seconds, consistent with what is shown by Fig: 6. The figure also shows that when the cycle length is less than optimal, the delay has higher values for the same range of the cycle length. For instance, if we compare the values for cycle length of 25 secs and 110 secs which are same distance from optimal cycle length 70 sec, the average delay value is about

22 secs/veh-mile and 26 secs/veh-mile approximately. The reason for this is that the curve is steeper in the left of the optimal cycle length.

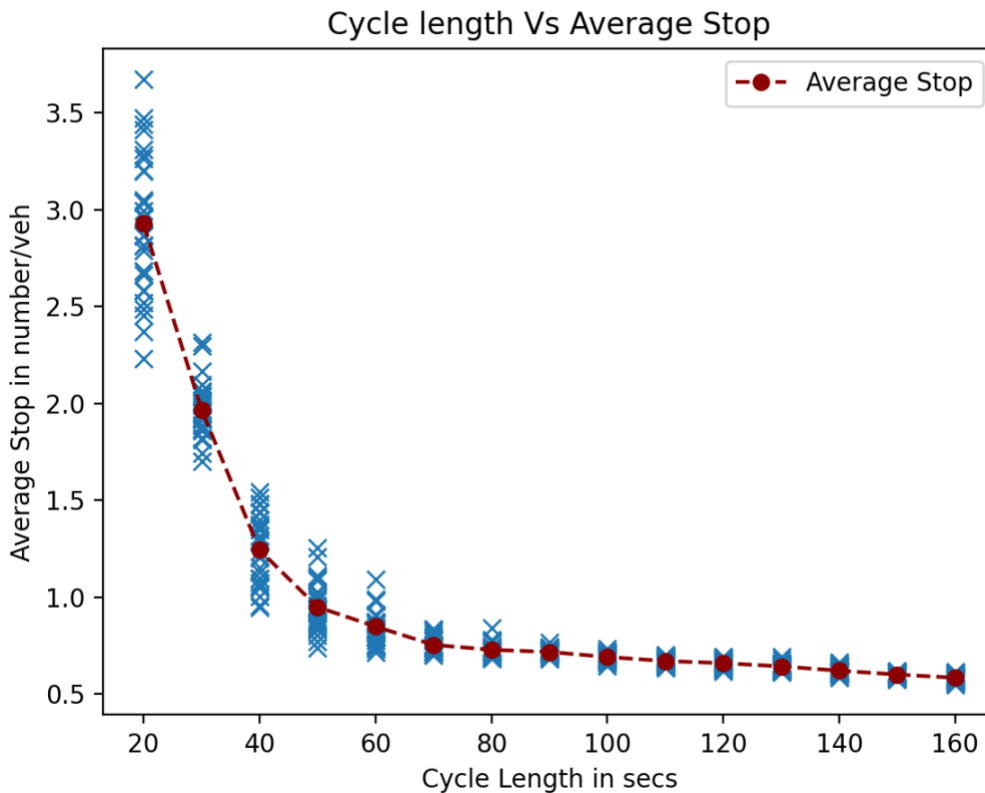


Fig: 7 Average stop rate in numbers/veh Vs Cycle Length

Fig:7 shows the relationship between cycle length and the average number of stops. At lower cycle lengths, the average no of stops per vehicle mile is very high because the vehicle needs to stop multiple times before passing through the intersection. Like delay, the average number of stops per vehicle mile at a lower cycle length is very high as the curve is steeper. Unlike delay, the average number of stops continues to decrease even after the webster optimal cycle length. When the cycle length is higher, a vehicle has to stop for a longer period, but the number of stops will be less.

## 4.2 Emission and Cycle Length

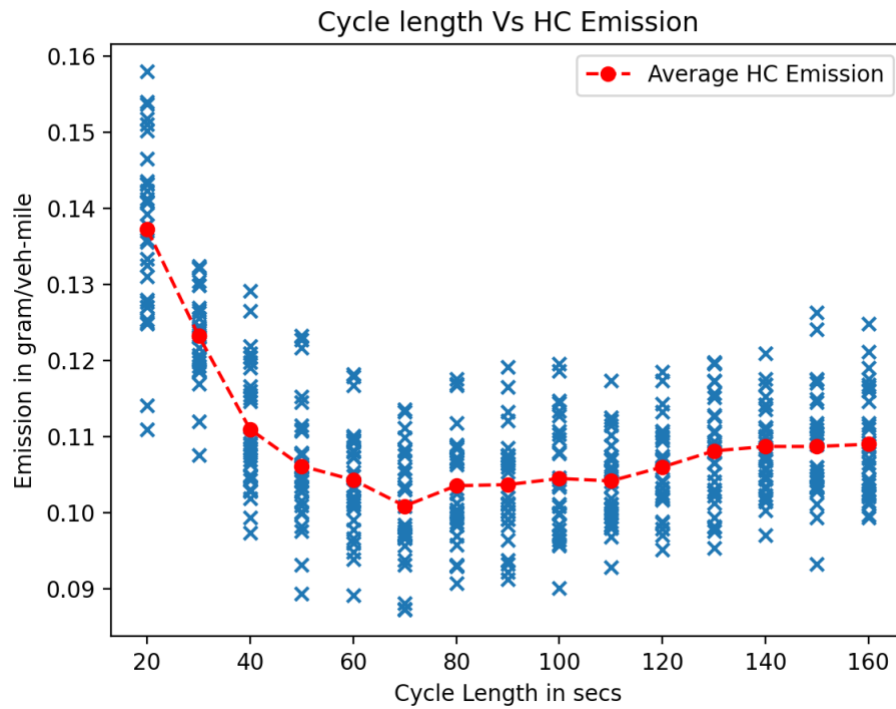


Fig: 8 Plot showing the HC emission in gram/veh-mile in each Cycle Lengths in seconds

Fig: 8 shows the plot between the HC emission at different cycle lengths. The average emission is highest at the cycle length of 20 seconds. The average emission then decreases with the increase in the cycle lengths until the webster's optimal cycle length (70 secs approx.). After that, the emission rate starts to increase gradually. The minimum value of the emission is about 0.10 grams/veh-mile at a cycle length of 70 secs. Even though the emission of HC increases after the optimal cycle length, the graph shows that the increment is not that significant.

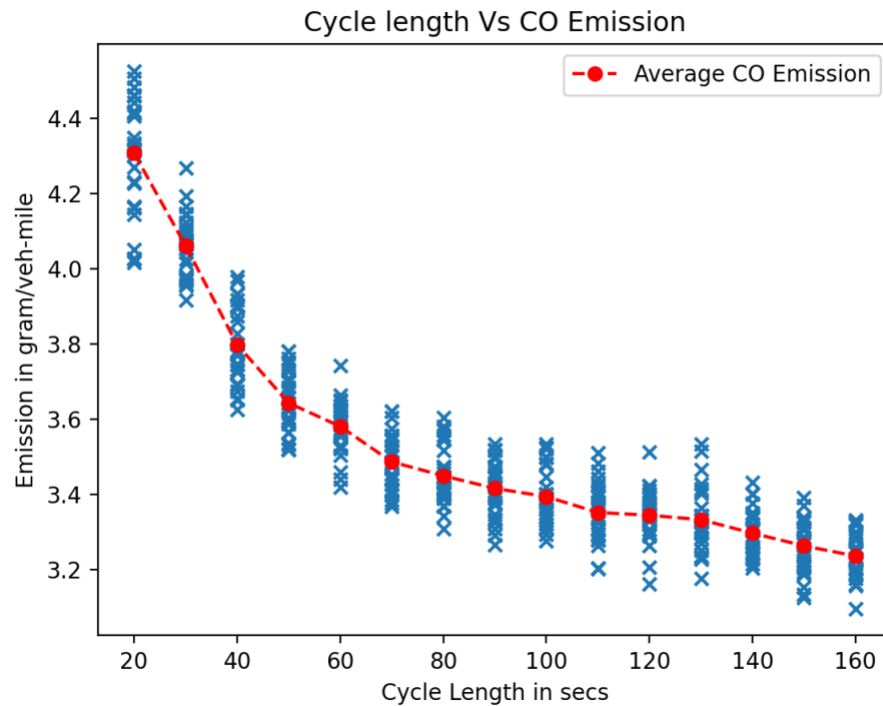


Fig: 9 Plot showing the CO emission in gram/veh-mile and Cycle Lengths in seconds

Fig:9 shows the plot of the Emissions of CO in grams/veh-mile and Cycle Lengths in seconds. CO emissions are very high at smaller cycle lengths and decrease rapidly up to the Webster's optimal cycle length (70 s). After the Webster's optimal cycle length, it continues to decrease but at a slower rate. The trend of CO emission rate with the Cycle length is similar to the trend of the acceleration, which could mean that the emission of CO is mostly related to the acceleration. This fact is also supported by the study conducted by Ritnar et al. The study found that acceleration emissions contributed more to total CO concentrations than a cruise or even idle emissions (Ritner, Westerlund, Cooper, & Claggett, 2013). The more the number of the stop, the more the proportions of the accelerations of all operations. The more the proportions of the accelerations, the more the emission of the carbon monoxides.

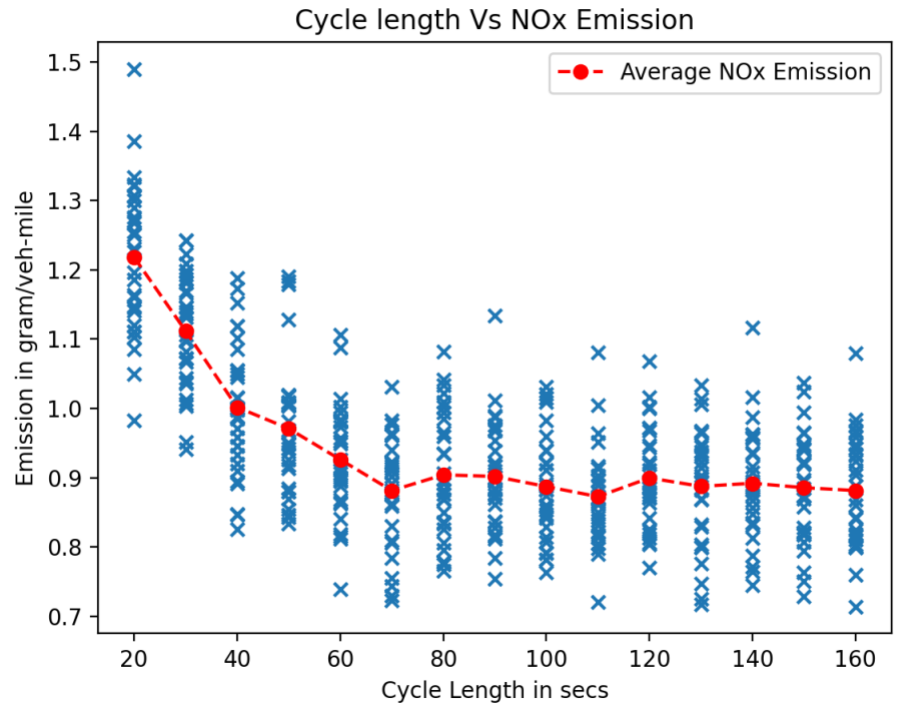


Fig: 10 Plot showing the NOx Emission in gram/vehicle-mile and Cycle Lengths in seconds

Fig: 10 shows the emissions of NOx in grams/veh-mile at different cycle lengths in seconds. The plot shows a similar trend as the plot for the CO emission. Like CO emissions, the NOx emission rate is very high at lower cycle lengths, and the curve flattens after the website's optimal cycle length. Unlike CO, the emission after Webster's optimal cycle length much flatter. Like CO, NOx is also produced mainly during acceleration when the temperature is high. The emission is lowest around the cycle length 70 secs and 110 secs, and the value is around 0.9 grams/veh-mile.

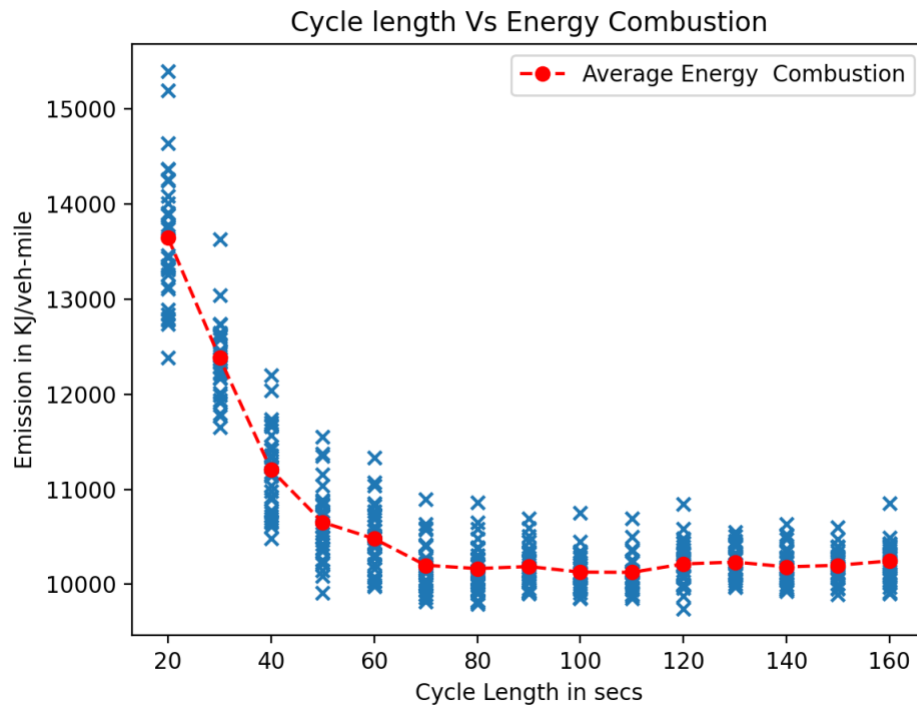


Fig: 11: Plot showing Energy consumption in KJ/veh-mile and Cycle Length in seconds

Fig: 11 shows the Energy consumption by the vehicles running in the intersection in KJ/veh-mile at different cycle lengths in seconds. The energy consumption is highest at the lowest cycle lengths. The emission rate decreases sharply until cycle length and decreases gradually until the cycle length of 100s.. The energy consumption is not much different from 70 secs to 160secs, and the value is about 10000 KJ/veh-mile.

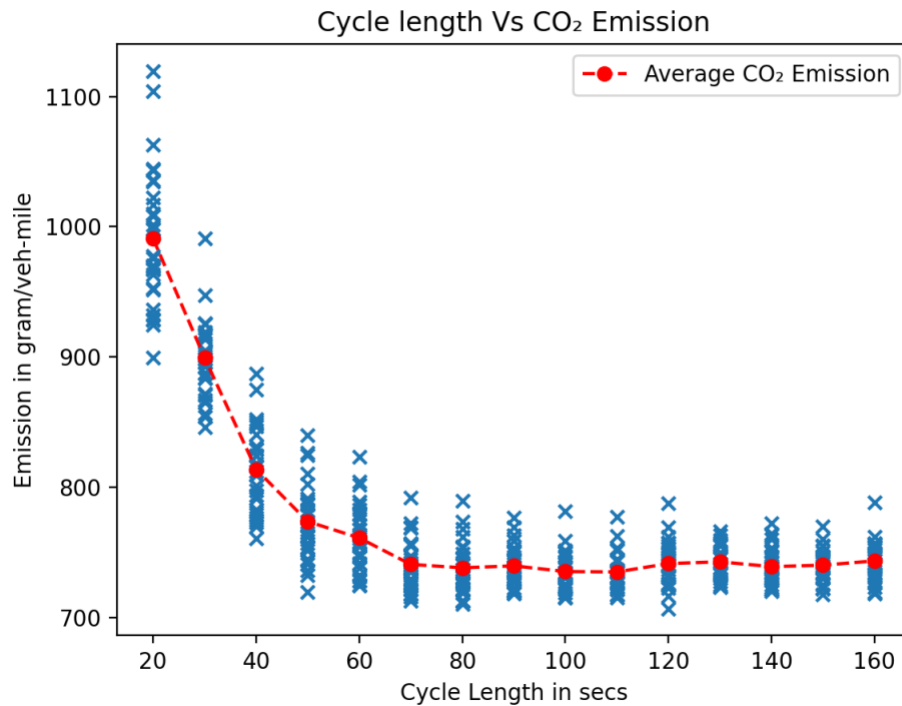


Fig: 12 Plot showing CO<sub>2</sub> in grams/veh-mile and Cycle Length in second

Fig: 12 shows average carbon dioxide (CO<sub>2</sub>) emission in grams/veh-mile at different Cycle lengths in seconds. The plot shows similar trends as that of energy consumption. The plot shows the highest emission at lower cycle length and has a minimum emission rate of 750 grams/veh-mile at 110 seconds, which could tell that the emission of CO<sub>2</sub> is directly related to the combustion of the fuel. Higher the rate of consumption of the fuel, the higher the rate of emission of the Carbon dioxide.

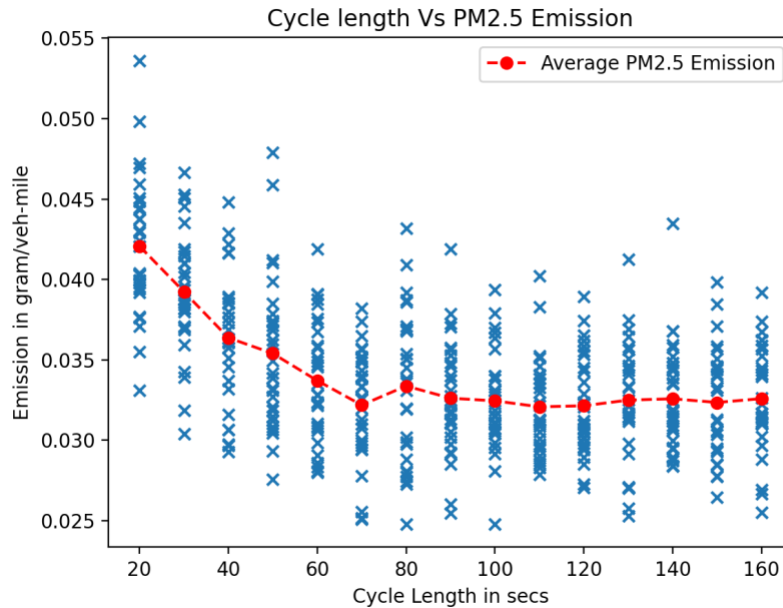


Fig: 13 Plot showing the PM2.5 emission rate in grams/veh-mile and Cycle Lengths in seconds

Fig:13 shows the plot of average PM 2.5 emission rates in grams/veh-mile at different cycle lengths in seconds. The rate is high at lower cycle lengths until the webster's optimal cycle length (70secs) is reached. After that, the plot is almost horizontal. The lowest emission rate is at 70secs, and the value is about 0.0325 gm/veh-mile..

Every type of pollutant has the highest emission rate in grams/veh-mile when the cycle length is 20 secs. Then the emission rate decreases with the increase of the cycle length. However, the decrease rate is different for each emission type. The cycle length for the lowest emission is also different. For instance, the emission of HC is lowest at the cycle length of 70 seconds, while the emission of CO is still decreasing even in 160 seconds.

Similarly, the lowest emission for the NO<sub>x</sub> is at 110 seconds. The energy combustion is lowest at the cycle length of 110 seconds. The CO<sub>2</sub> emission is lowest as the cycle length

of 110s as well. The cycle length with the lowest emission of PM<sub>2.5</sub> is 110 seconds. It is also observed that the emission of CO decreases gradually with the cycle length. In contrast, emission for other pollutants decreases abruptly at low cycle length and decreases or increases at a slower rate for the higher cycle lengths. The value of the lowest cycle length for each pollutant is summarized in the table below. Values of the lowest cycle length for each pollutant is summarized in the table below.

While emission rate for every pollutant is decreasing until the webster's optimal cycle length and beyond webster's optimal cycle length the increase/decrease is different for different pollutant type. In this case, it is better to decide a optimal range of cycle length rather than a optimal cycle and the optimal range should start with a cycle length of 70 seconds. Considering 120 s as practical upper limit (Zakariya & Rabia, 2016)), the optimal range of cycle length for each pollutant is shown if Table 3 below.

Table 3: Minimum emission of Pollutants and Cycle Length

SN	Pollutant	Emission rate gm/veh-mile	Cycle Length seconds
1	Hydrocarbon (HC)	0.101 - 0.105	70 s-110 s
2	Carbon monoxide (CO)	3.38 - 3.42	100 s-120 s
3	Nitrogen Oxide (NO <sub>x</sub> )	0.88 - 0.92	70 s-110 s
5	Carbon dioxide (CO <sub>2</sub> )	730 -740	70 s-120 s
6	Particulate Matter (PM <sub>2.5</sub> )	0.032-0.034	70 s -120 s

### 4.3 Variation of Emission Rate by Vehicle Type with Cycle Length

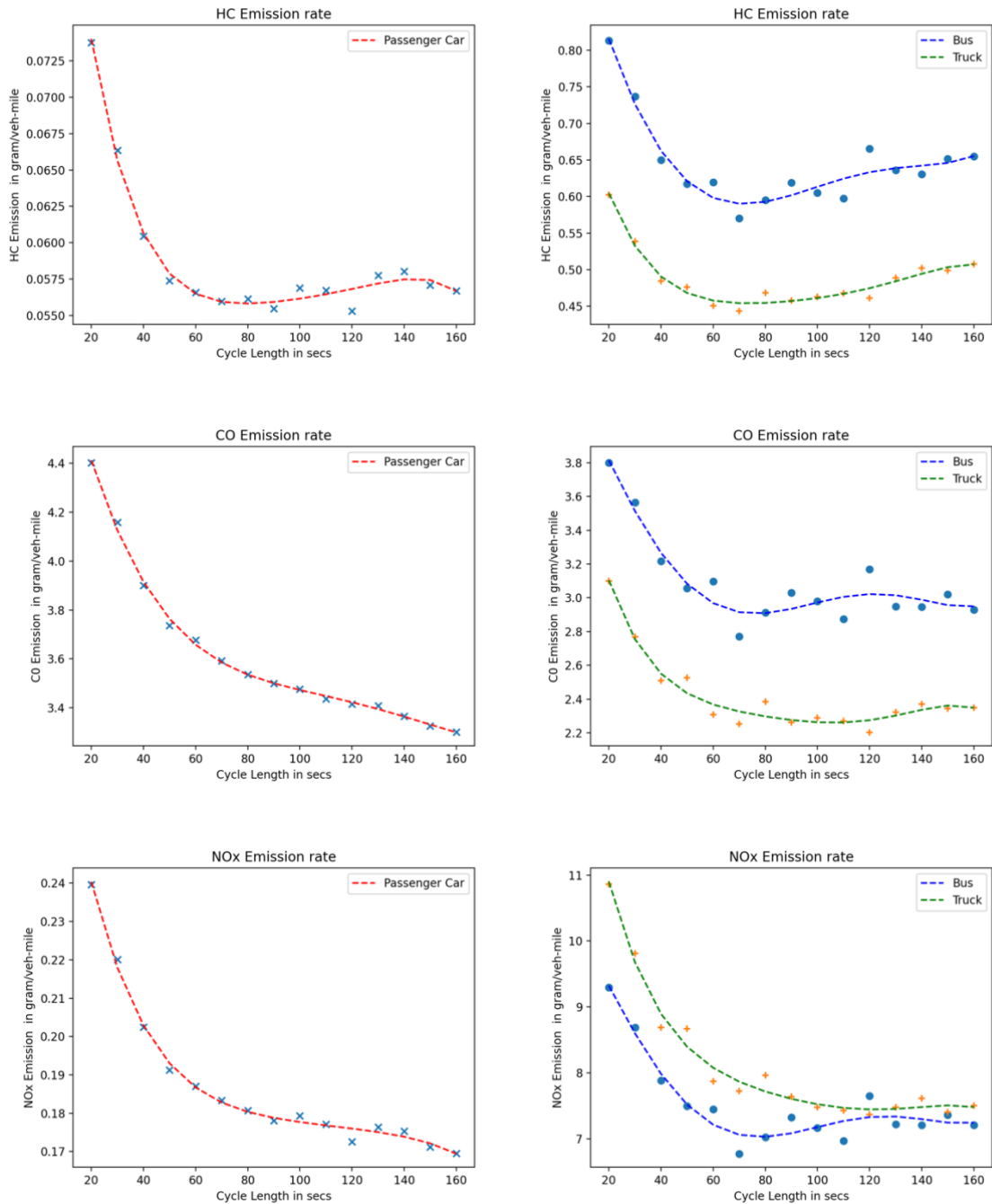


Fig: 14: Emission rate at different cycle length for different vehicle type for HC, CO, and NOx

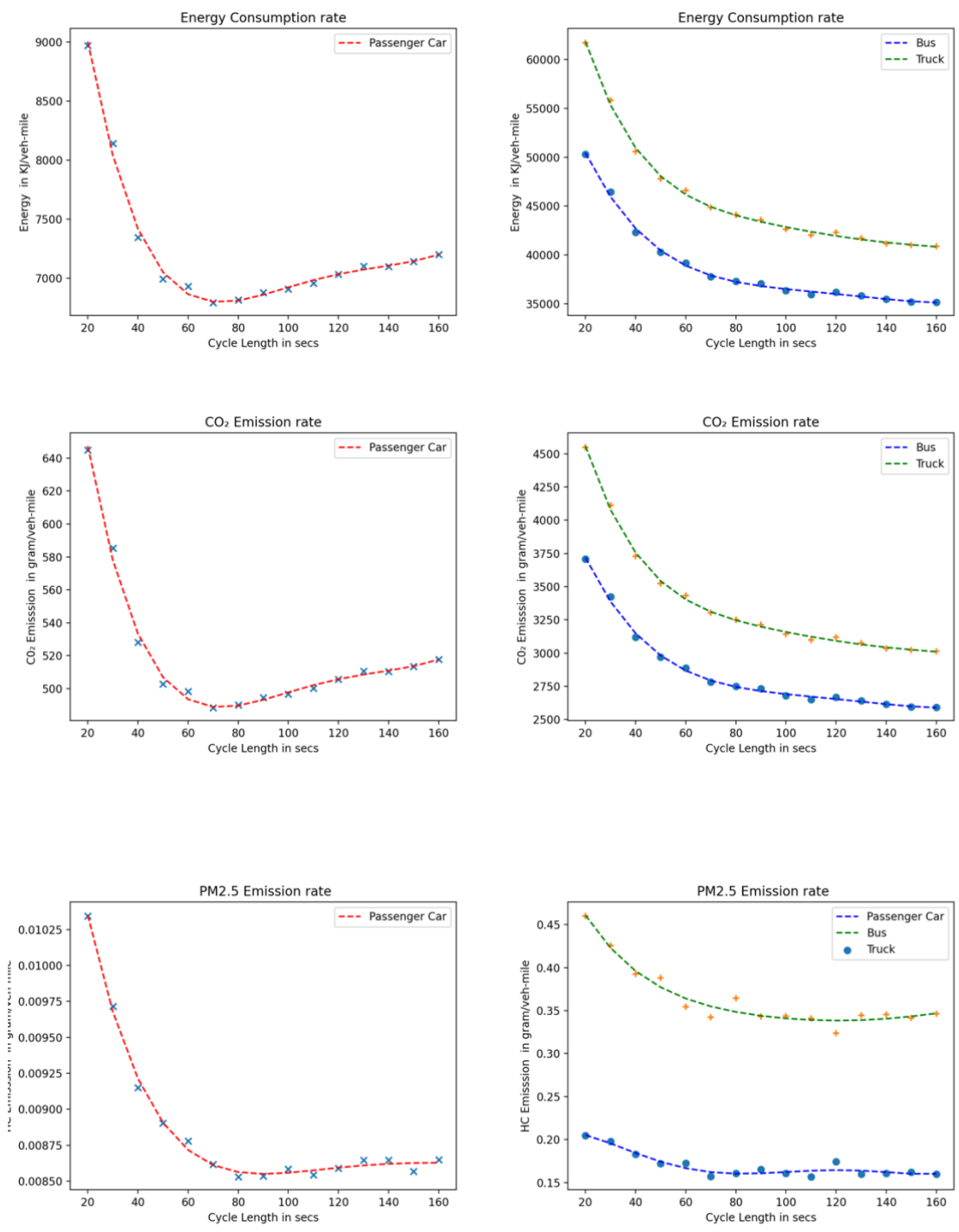


Fig: 15 Emission rate at different cycle length for different vehicle type for energy consumption, CO<sub>2</sub> and PM2.5

Fig: 14-15 shows the emission rates of emission in grams/veh-mile for each vehicle type at different cycle lengths. We can see that different pollutant have different trends, and also, different vehicle types have different emission rate trends with the cycle length. Different pollutants have different lowest emission cycle lengths. Moreover, the different vehicle type has different optimal cycle lengths. We can know from the graph for HC that the bus has a higher emission rate than that of the truck. The car has the lowest HC emission rate. The emission rate of CO is higher for the vehicle type car (using gasoline) than bus (using diesel) and trucks (diesel) as shown in fig: 14. “The fuel for cars is gasoline, which is a compound of 85 % carbon and 15 % hydrogen; so, the emissions of cars are major composed of CO and HC” (Chen & Yu, 2007). Therefore, we can conclude that the nature of the curve for CO emission rate at different cycle length is also mostly contributed by the emission from the cars. Similarly, “Diesel engine uses compression ignition rather than the spark ignition used in petrol engines and operates with a lower fuel to air ratio than petrol engines using lean burning fuel and air mixtures, which result in higher emissions of NO<sub>x</sub>” (Mardsen, Bell, & Reynolds, 2001). Therefore, the major contribution of the NO<sub>x</sub> is from trucks and buses. Also, Except CO, the emission rate is highest for the truck and lowest for the car. For the pollutants, HC, CO<sub>2</sub>, and PM 2.5 lowest emission rate for car is the cycle length 60-100 secs. In the case of trucks and buses, the lowest emission rate is for the higher cycle lengths.

#### 4.4 Variation of Proportion of Operation with Cycle Length

The vehicle operations for a vehicle traveling in the roadway can be classified as acceleration, cruise, deceleration, and idle. In the case of a signalized intersection, the vehicle accelerates when the vehicle is at a stop, and the light turns green. After some time

on the road, it attains the speed limit and starts to move at a constant speed called cruise. The vehicle begins to decelerate when it approaches the red light in the intersection; this operation is called deceleration and comes to a complete stop called idle. The vehicle engine is assumed to be always on, even when it is idle. Therefore, in each operation, there is a significant amount of emission of each pollutant.

The output file from the simulation of VISSIM contains the value of speed and acceleration for each second. We can categorize if the vehicle in each second is on the acceleration, deceleration, cruise, or idle from the speed and acceleration. The following criteria are used for classifying the operation.

Table 4: The categories of the vehicle operation mode

SN	Operation	Criteria for speed <b>mph</b>	Criteria for acceleration <b>mph/s</b>
1	Deceleration		$(a_{t-2} < -1 \text{ AND } a_{t-1} < -1 \text{ AND } a_t \leq -1)$ OR $(a_t < -2)$
2	Idle	$-1 \leq v_t < 1$	Any
3	Cruise	Any	$a_t \leq 2$
4	Acceleration	Any	$a_t > 2$

The criteria should be used in the order listed on the Table 4. This means that the criteria must be checked for deceleration first and then idle and the cruise and finally for acceleration.

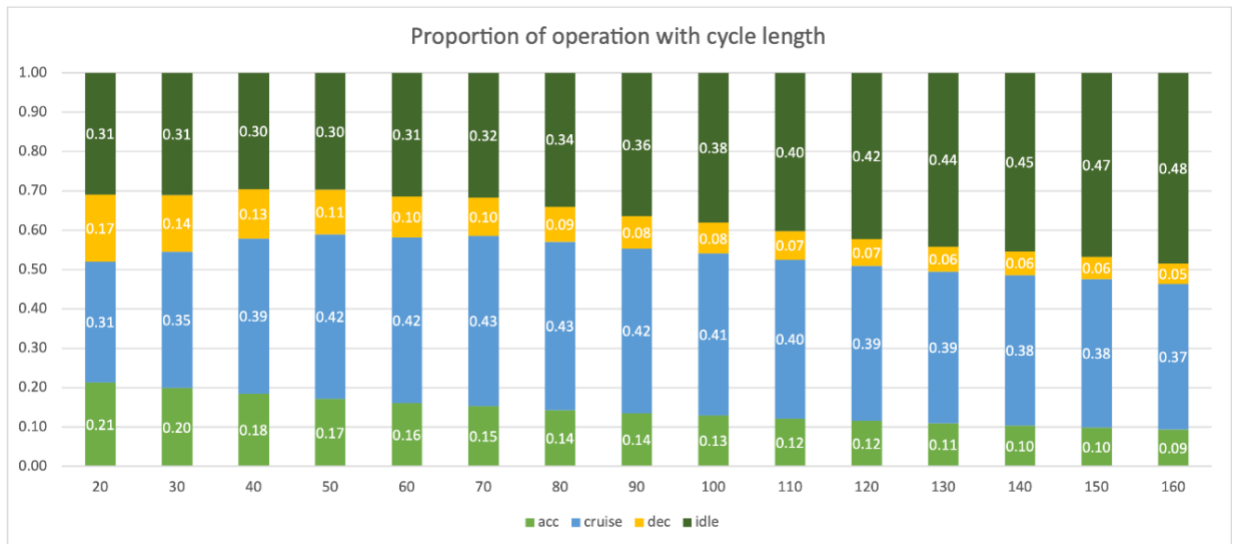


Fig: 16 Variation of Proportion of Operations with Cycle Length

Fig:16 shows the variation of vehicle operating modes with the cycle lengths. As seen in the figure, the proportion of acceleration decrease with an increase in the cycle length because with an increase in the cycle length, the stoppings are few, as shown in the plot of stopping vs. cycle length in fig: 7. When stopping is less, most of the time, the vehicle can run at a constant speed. The proportion for the cruise is maximum at cycle length 70 secs (which is near to optimal cycle length) and decreases both left and right of the cycle length 70 seconds because it is related to delay. At optimal cycle length, the most proportion of the vehicle travel is in a cruise. The decrement is gradual at the right of the webster's optimal cycle length and rapid on the left. For the deceleration, it decreases with the increase of the cycle length. The reason is that with the increase in cycle length, the stopping is decreased. Thus, the vehicle does not have to stop too many times. The proportion of idle is opposite to that of the cruise. It is minimum at the optimal cycle length as the delay is optimized. It is highest at the higher and lower cycle length. At higher cycle length, the proportion of idle is high because of the high stopping time or high delay.

### 4.5 Proportion of the vehicle Operations and proportion of the Emissions

The Fig:17-22 shows the proportion of emission by operating modes: acceleration, cruise, deceleration, and idle for each type of pollutants. The proportion differs for each type of pollutants. The figures show that in each pollutant type, the proportion of emission from acceleration and deceleration decreases with increase in cycle length and the proportion of emission from cruise increases with increases in the cycle length. However, the increment of proportion of cruise with cycle length after the cycle length of 70 secs is significantly less to no increment. The proportion of emission from the idle decrease until the cycle length of 50 secs and start increasing after that.

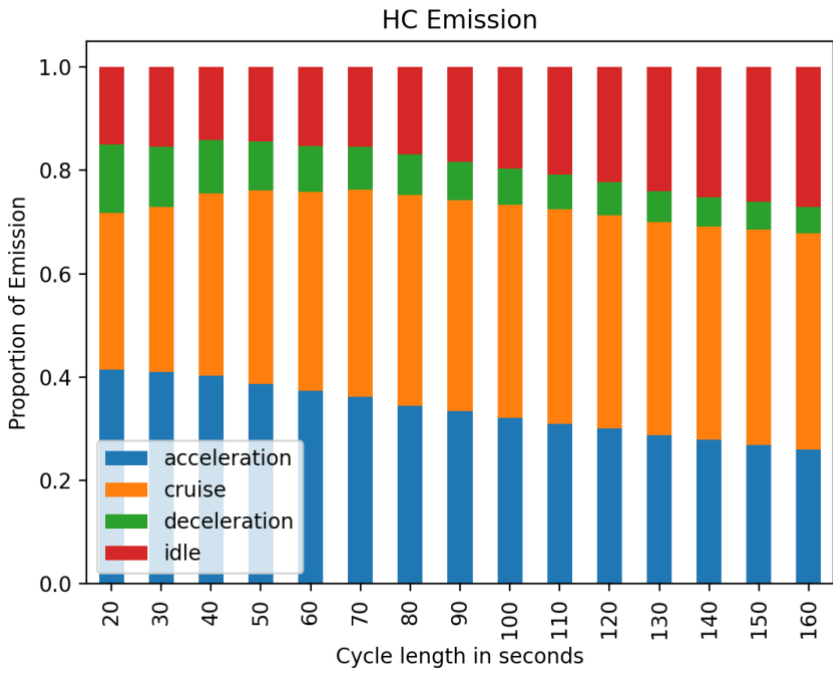


Fig: 17 Proportion of HC Emission by travel time in operation at different Cycle Length

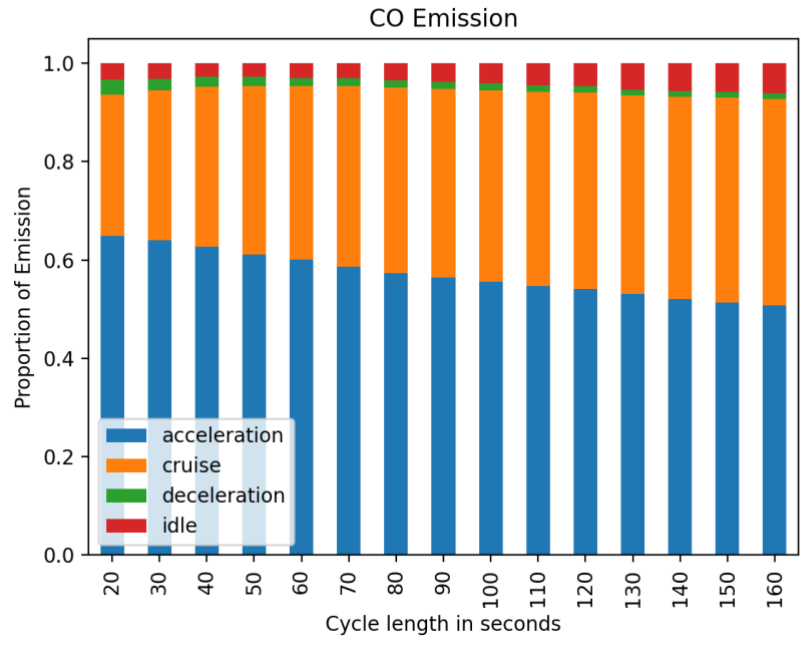


Fig: 18 Proportion of CO Emission by Operation at different Cycle Length

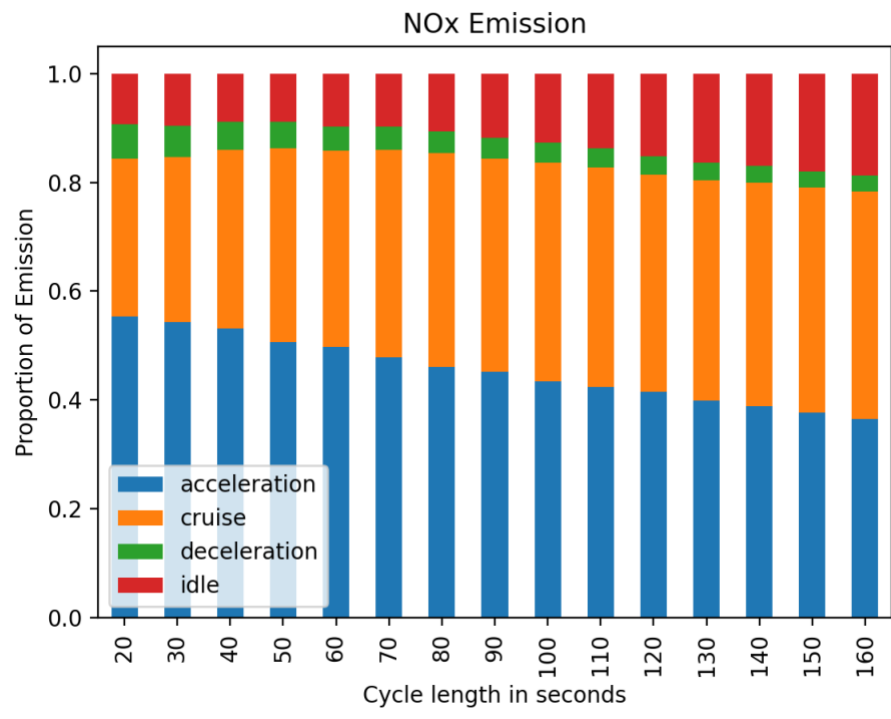


Fig: 19 Proportion of NOx Emission by Operation at different Cycle Length

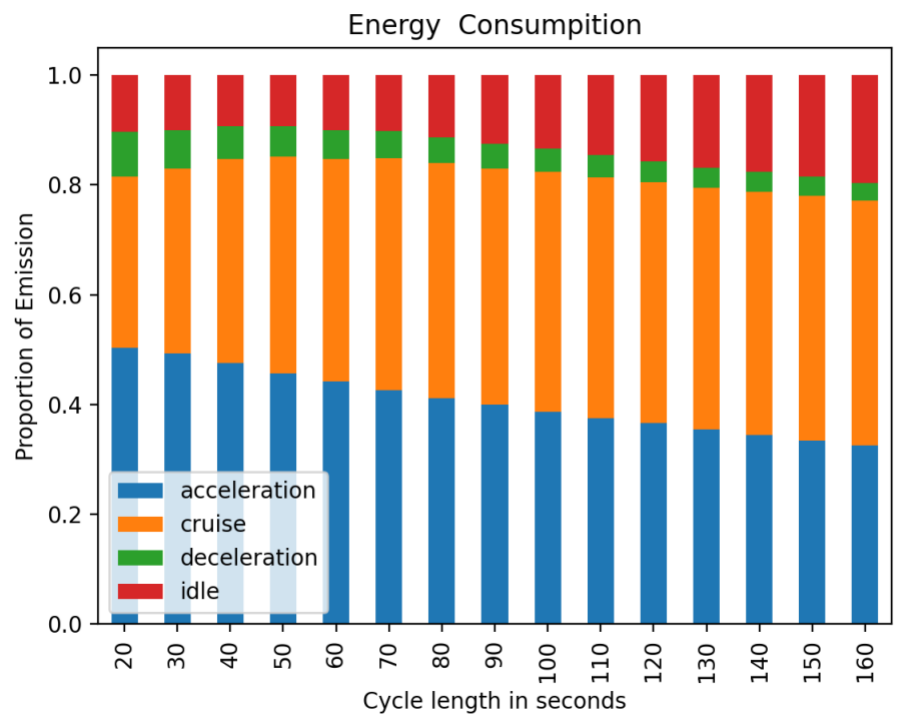


Fig: 20 Proportion of Energy Consumption by Operation at different Cycle Length

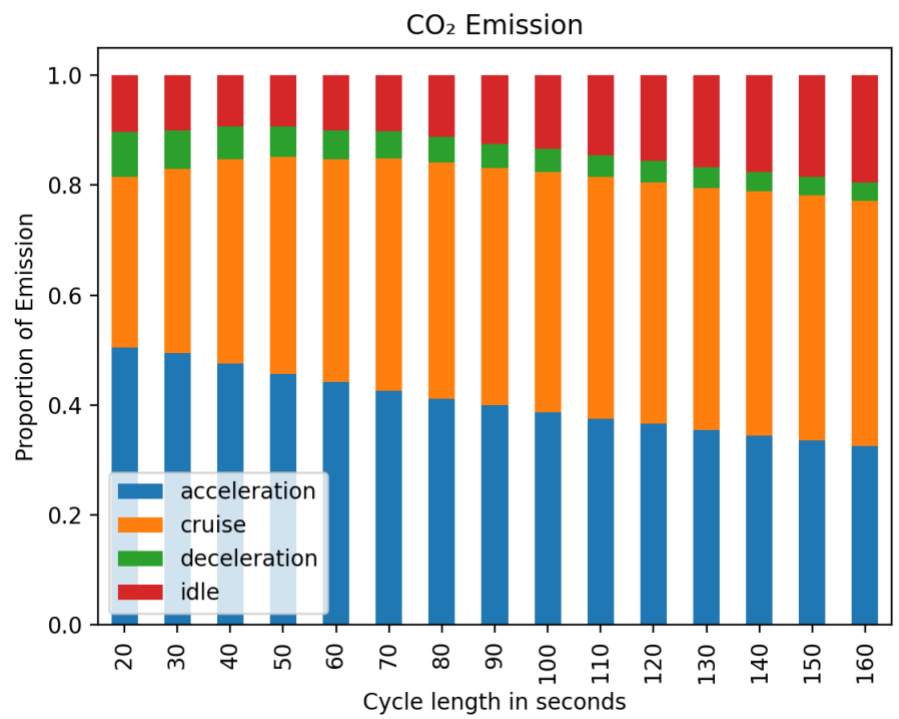


Fig: 21 Proportion of CO2 Emission by Operation at different Cycle Length

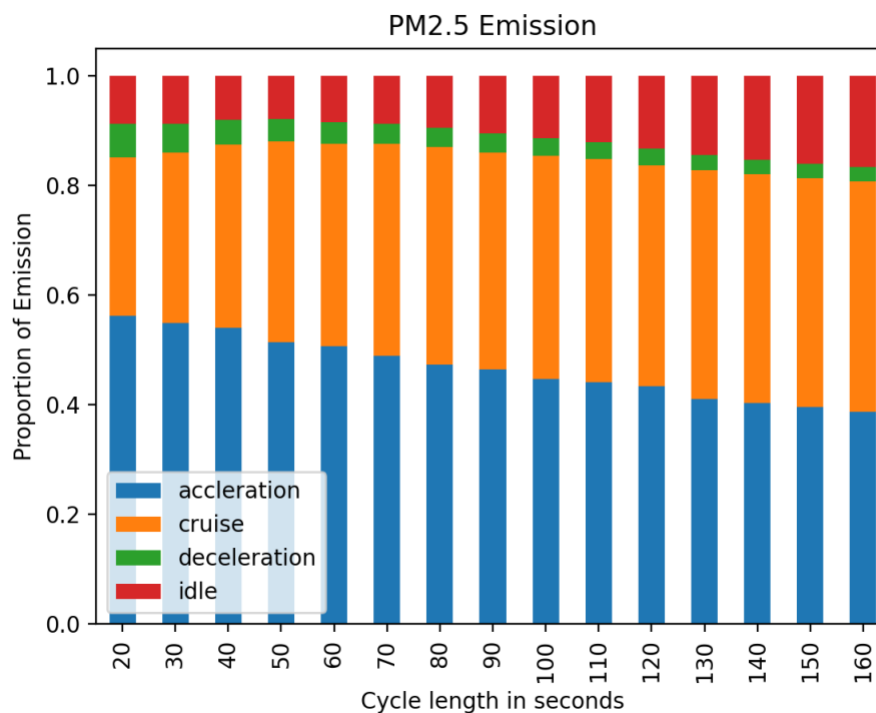


Fig: 22 Proportion of PM2.5 Emission by Operation at different Cycle Length

In all the figures, the major contribution for the emission is from the acceleration and then by the cruise. The idle and the deceleration contribute significantly less to the emission. In the case of Carbon monoxide, it can be seen that the emission is high for acceleration. The amount of CO emission from the cruise is almost identical. In webster's optimal cycle length (70 secs) the amount of emission from acceleration is almost 60%. However, the amount of CO emission from the idle and deceleration is low compared to other pollutants which less than 5%. The proportion of emission for webster's cycle length and webster's cycle length is summarized in the table below.

Table 5: Proportions of operating modes at webster's optimal cycle length and optimal cycle length for emission

SN	Pollutant	Emission Proportion at Webster's Optimal cycle length (70s)		Emission Proportion at Optimal cycle length for emission (110s)	
1	HC	Acceleration:	0.36	Acceleration:	0.31
		Cruise:	0.41	Cruise:	0.42
		Deceleration:	0.08	Deceleration:	0.06
		Idle:	0.15	Idle:	0.21
2	CO	Acceleration:	0.59	Acceleration:	0.55
		Cruise:	0.36	Cruise:	0.40
		Deceleration:	0.02	Deceleration:	0.01
		Idle:	0.03	Idle:	0.04
3	NOx	Acceleration:	0.48	Acceleration:	0.42
		Cruise:	0.38	Cruise:	0.40
		Deceleration:	0.04	Deceleration:	0.04
		Idle:	0.10	Idle:	0.14
4	Energy	Acceleration:	0.43	Acceleration:	0.37
		Cruise:	0.42	Cruise:	0.44
		Deceleration:	0.05	Deceleration:	0.04
		Idle:	0.10	Idle:	0.14
5	CO <sub>2</sub>	Acceleration:	0.43	Acceleration:	0.37
		Cruise:	0.42	Cruise:	0.44
		Deceleration:	0.05	Deceleration:	0.04
		Idle:	0.10	Idle:	0.14
6	PM2.5	Acceleration:	0.49	Acceleration:	0.44
		Cruise:	0.40	Cruise:	0.41
		Deceleration:	0.05	Deceleration:	0.03
		Idle:	0.08	Idle:	0.12

Changing the cycle length from the webster's optimal cycle length to the higher cycle length for emission leads to a decrease in emission due to acceleration and an increase in the emission due to idle in most pollutants. Similarly, this will lead to an increase in the proportion of mainly idle and sometimes cruise. This is because when we increase the cycle length, the delay increases, which means stopping time is increased. Thus, the proportion of the idle is also increased, which thereby increase emission due to idle. However, this is

different in the case of CO. In the case of CO, the proportion of emissions due to cruise increased. This is because the proportion of emissions due to idle is already very low.

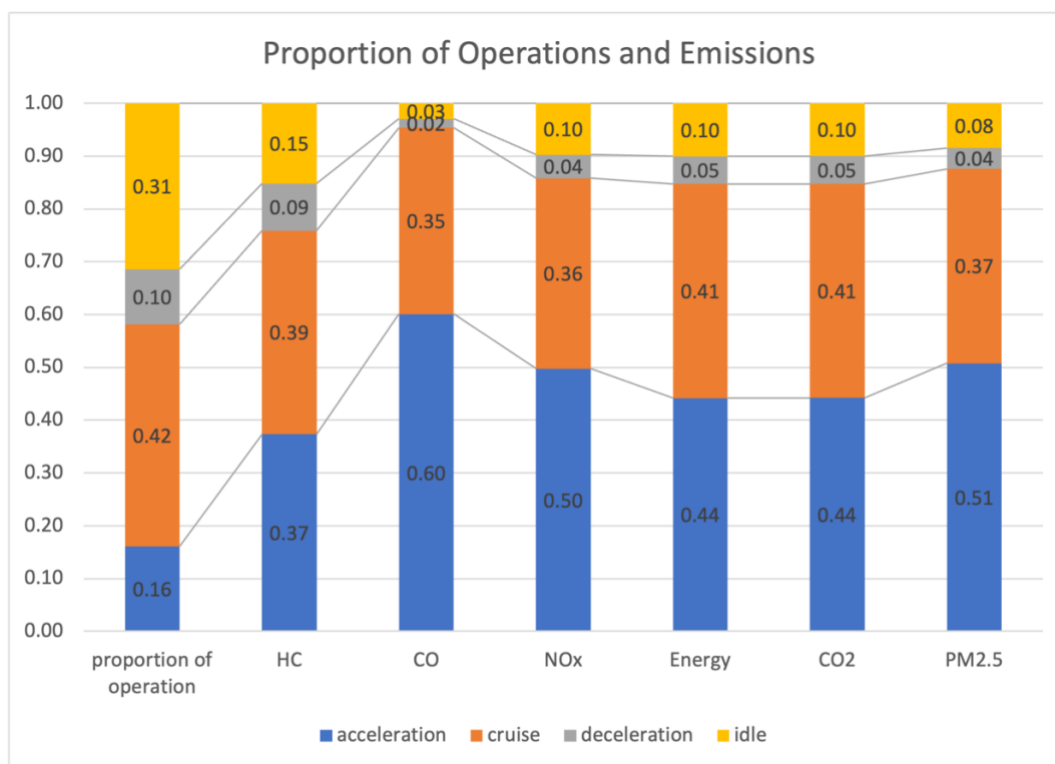


Fig: 23: Proportion of operating modes and Emissions

Fig:23 shows a comparison of the proportion of operating modes and proportion of emission in each operation mode for each type of pollutant under study. Except for HC, the proportion of emission from acceleration is highest for all types of pollutants even though the proportion of the acceleration is just 0.16 percent. The proportion of emission for every pollutant is almost the same as the proportion of the cruise. The proportion of emission due to deceleration is significantly less for every kind of pollution except for HC, where the proportion is nearly the same.

The proportion of emission by vehicles during idle is very less. The proportion of CO emissions is highest due to acceleration and the proportion of emission due to deceleration and idle are very low.

### 4.6 Proportion of Vehicles and Proportion of Emission

For this study, the composition of the vehicle chosen is car 90%, bus 5%, and truck 5%. However, the emission of different pollutants is not in the same proportions as the vehicle type proportion, as shown in Fig: 23.

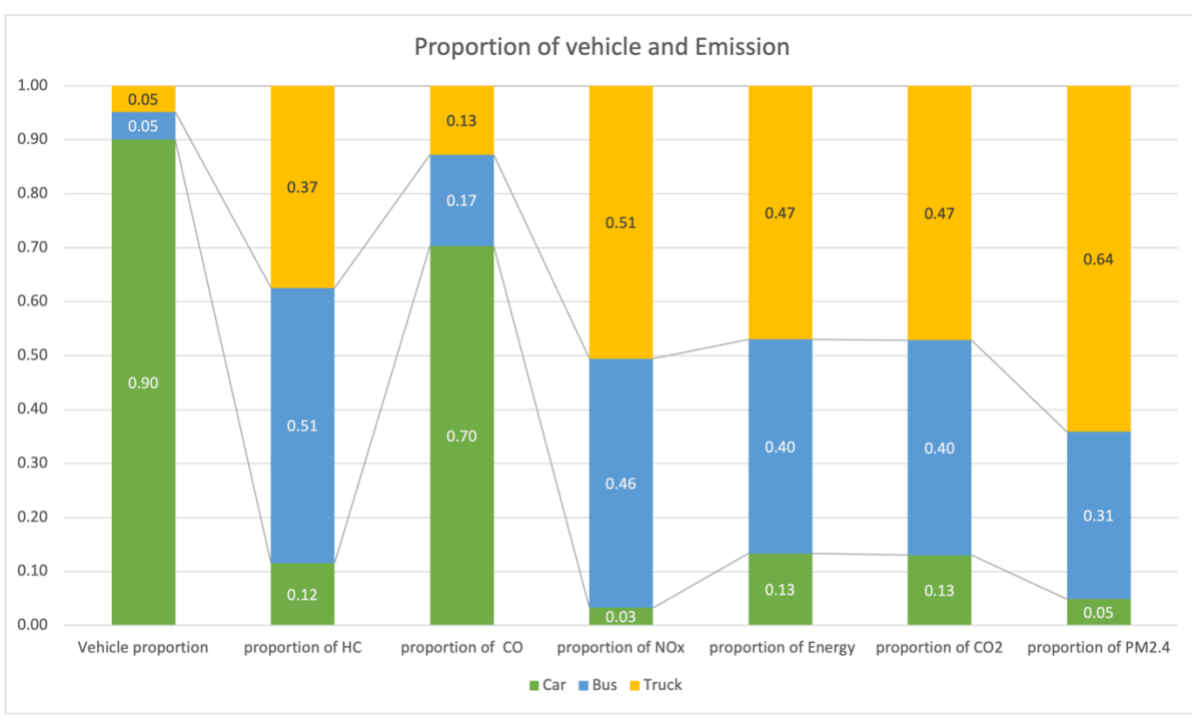


Fig: 24 Proportions of vehicles and emissions

Fig: 24 shows the proportions of Emissions of pollutants compared to the proportion of the vehicle compositions. Even though 90% of the vehicles are cars, the emissions of Hydrocarbon, Nitrogen oxide, energy combustion, Carbon dioxide, and PM2.5 are very

low compared to the amount of emissions by the bus and trucks. The bus and truck combined contribute to almost more than 90% of the emissions. The exception is in the Carbon monoxide case where the emission from the car is 70%. This is because the emission rate of CO from car is higher than from trucks and bus and there is more proportion cars; therefore, the proportion of emission of CO from cars is significantly higher than the emissions for trucks and bus.

## 4.7 Regression Analysis

Finally, regression analysis is carried out to determine if there is a correlation between Pollutant emission rate in grams/veh-mile with cycle length in seconds, delay rate in seconds/veh-mile, and stopping rate in number/veh-mile. Regression is carried out for each pollutant; therefore, total 6 regression is carried out.

### 4.7.1 Regression between HC emission rate and Cycle length, average delay and average stop

The figure below shows the plot between HC emission rate (Pollutant\_1) and Cycle length; HC emission rate and average; and delay and average stop.

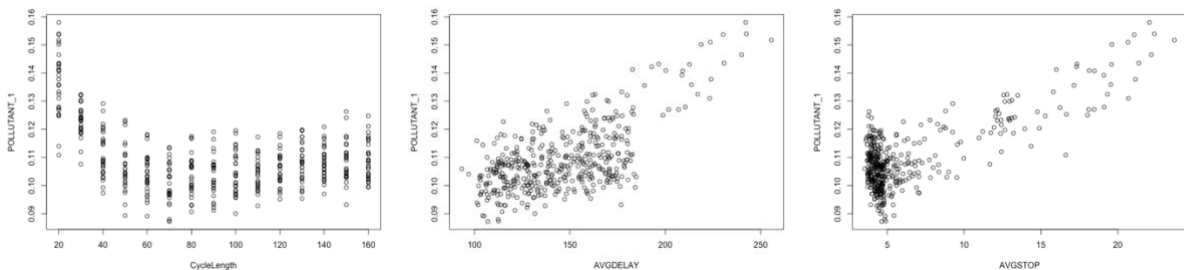


Fig: 25 Plot for HC with Cycle Length, Average delay, and Average stop

Residuals:

	Min	1Q	Median	3Q	Max
	-0.0193065	-0.0046063	-0.0005904	0.0048610	0.0175360

Coefficients:

	Estimate	Std. Error	t value	Pr(> t )
(Intercept)	7.851e-02	1.861e-03	42.184	< 2e-16 ***
CycleLength	-7.913e-05	5.341e-05	-1.482	0.139154
AVGDELAY	2.298e-04	6.713e-05	3.423	0.000676 ***
AVGSTOP	6.893e-04	6.589e-04	1.046	0.296030

---

Signif. codes: 0 '\*\*\*' 0.001 '\*\*' 0.01 '\*' 0.05 '.' 0.1 ' ' 1

Residual standard error: 0.006745 on 446 degrees of freedom

Multiple R-squared: 0.6602, Adjusted R-squared: 0.6579

F-statistic: 288.8 on 3 and 446 DF, p-value: < 2.2e-16

Fig: 26: Result of Regression for Pollutant 1(HC)

This regression shows that the relationship between Hydrocarbon emission rate is statistically significant with average delay only and not significant with cycle length and average stop. Also, looking at the adjusted R-squared value is low; therefore, the relationship is not significant between these variables.

#### 4.7.2 Regression between CO emission rate and Cycle length, average delay and average stop

The fig: 26 shows the plot for CO (Pollutant 2) with Cycle length, Average delay and Average stop.

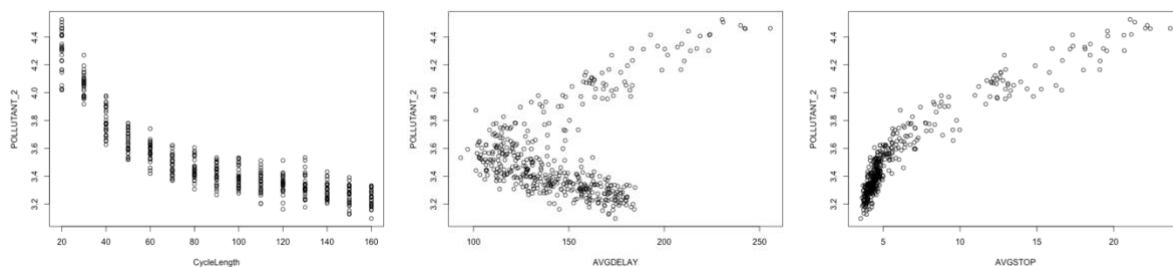


Fig: 27 Plot for CO with Cycle Length, Average delay, and Average stop

The result of the regression is shown below:

```

Residuals:
      Min       1Q   Median       3Q      Max
-0.208441 -0.050377  0.000519  0.052227  0.229976

Coefficients:
              Estimate Std. Error t value Pr(>|t|)
(Intercept)  3.4098376  0.0210165 162.246 < 2e-16 ***
CycleLength -0.0056251  0.0006032  -9.326 < 2e-16 ***
AVGDELAY      0.0037260  0.0007581   4.915 1.25e-06 ***
AVGSTOP       0.0134136  0.0074407   1.803  0.0721 .
---
Signif. codes:  0 '***' 0.001 '**' 0.01 '*' 0.05 '.' 0.1 ' ' 1

Residual standard error: 0.07618 on 446 degrees of freedom
Multiple R-squared:  0.9395,    Adjusted R-squared:  0.939
F-statistic: 2307 on 3 and 446 DF,  p-value: < 2.2e-16

```

Fig: 28 Result of Regression for Pollutant 2 (CO)

This regression shows that the relationship between Carbon monoxide emission rate is statistically significant with cycle length and average delay but not significant with average stop. Looking at the adjusted R-squared value, which is very high the relationship is significant.

#### 4.7.3 Regression between NOx emission rate and Cycle length, average delay and average stop

The fig: 28 shows the plot for NOx (Pollutant 3) with Cycle length, Average delay and Average stop.

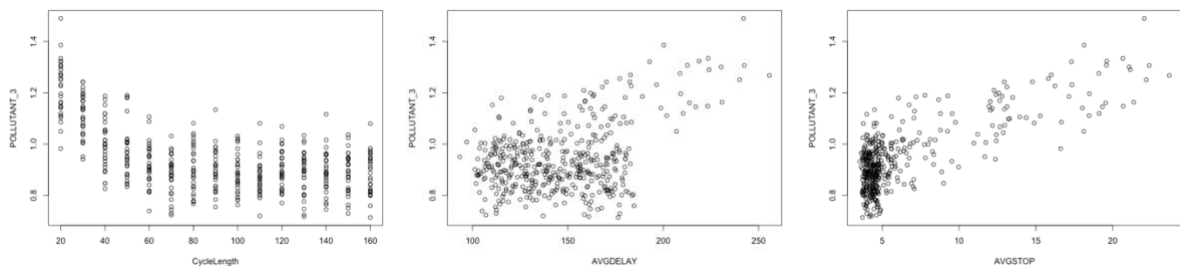


Fig: 29 Plot for NOx with Cycle Length, Average delay, and Average stop

The result of the regression is shown below:

```

Residuals:
      Min       1Q   Median       3Q      Max
-0.185400 -0.061396 -0.000507  0.059524  0.233169

Coefficients:
              Estimate Std. Error t value Pr(>|t|)
(Intercept)  0.7865343  0.0227334  34.598  <2e-16 ***
CycleLength -0.0015415  0.0006525  -2.363  0.0186 *
AVGDELAY     0.0017881  0.0008201   2.180  0.0297 *
AVGSTOP     0.0052150  0.0080486   0.648  0.5174
---
Signif. codes:  0 '***' 0.001 '**' 0.01 '*' 0.05 '.' 0.1 ' ' 1

Residual standard error: 0.0824 on 446 degrees of freedom
Multiple R-squared:  0.5836,    Adjusted R-squared:  0.5808
F-statistic: 208.4 on 3 and 446 DF,  p-value: < 2.2e-16

```

Fig: 30 Result of Regression for Pollutant 3 (NOx)

This regression shows that the relationship between NOx emission rate is statistically significant with cycle length and average delay but not significant with average stop. Looking at the adjusted R-squared value, which is low, they are not strongly correlated.

#### 4.7.4 Regression between Energy Consumption rate and Cycle length, average delay and average stop

The fig: 30 below shows the plot for the Energy consumption rate with Cycle length, Averaged delay and Average stop.

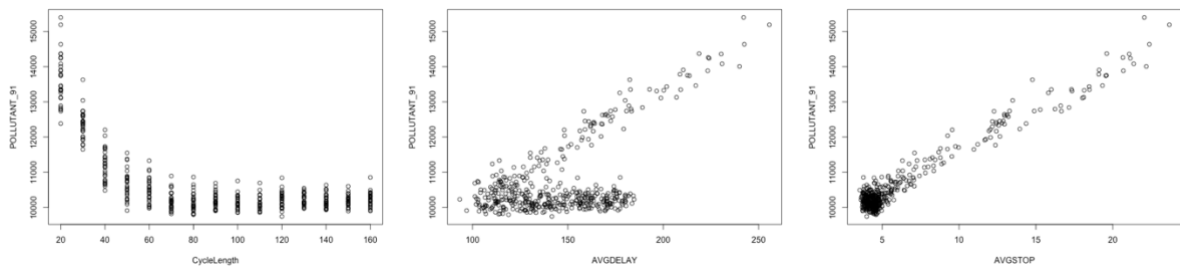


Fig: 31 Plot for Energy with Cycle Length, Average delay, and Average stop

The result of regression is shown below:

```

Residuals:
  Min       1Q   Median       3Q      Max
-537.95 -147.84  -24.46  117.25  830.40

Coefficients:
              Estimate Std. Error t value Pr(>|t|)
(Intercept)  8581.287    58.245  147.332 <2e-16 ***
CycleLength  -16.126     1.672   -9.647 <2e-16 ***
AVGDELAY      22.759     2.101   10.832 <2e-16 ***
AVGSTOP       37.186     20.621   1.803  0.072 .
---
Signif. codes:  0 '***' 0.001 '**' 0.01 '*' 0.05 '.' 0.1 ' ' 1

Residual standard error: 211.1 on 446 degrees of freedom
Multiple R-squared:  0.9584,    Adjusted R-squared:  0.9581
F-statistic: 3426 on 3 and 446 DF,  p-value: < 2.2e-16
    
```

Fig: 32 Result of Regression for Pollutant 3 (Energy)

This regression analysis shows that the energy consumption rate is statistically significant with cycle length and average delay but not significant with average stop. Looking at the adjusted R-squared value, which is high, the consumption rate is strongly correlated with cycle length, average delay, and average stop.

#### 4.7.5 Regression between CO<sub>2</sub> emission rate and Cycle length, average delay and average stop

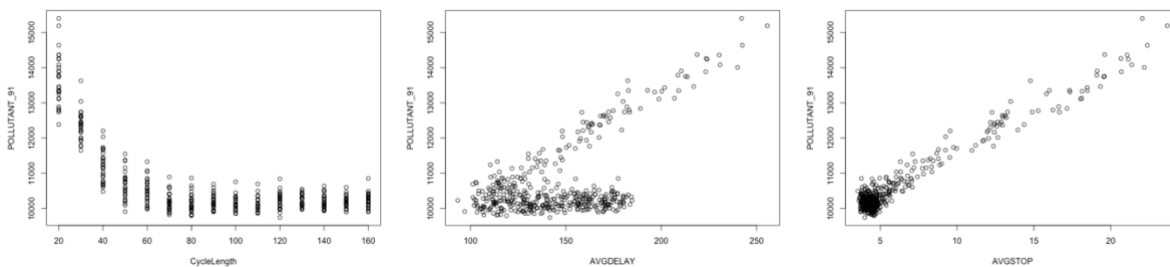


Fig: 33 Plot for CO<sub>2</sub> emission with Cycle Length, Average delay, and Average stop

The result for the regression is below:

Residuals:

	Min	1Q	Median	3Q	Max
	-537.95	-147.84	-24.46	117.25	830.40

Coefficients:

	Estimate	Std. Error	t value	Pr(> t )	
(Intercept)	8581.287	58.245	147.332	<2e-16	***
CycleLength	-16.126	1.672	-9.647	<2e-16	***
AVGDELAY	22.759	2.101	10.832	<2e-16	***
AVGSTOP	37.186	20.621	1.803	0.072	.

---

Signif. codes: 0 '\*\*\*' 0.001 '\*\*' 0.01 '\*' 0.05 '.' 0.1 ' ' 1

Residual standard error: 211.1 on 446 degrees of freedom

Multiple R-squared: 0.9584, Adjusted R-squared: 0.9581

F-statistic: 3426 on 3 and 446 DF, p-value: < 2.2e-16

Fig: 34 Result of Regression for Pollutant 98 (CO<sub>2</sub>)

This regression analysis shows that the CO<sub>2</sub> emission rate is statistically significant with cycle length and average delay but not significant with average stop. Looking at the adjusted R-squared value, which is high, the emission rate is strongly correlated with cycle length, average delay, and average stop.

#### 4.7.6 Regression between PM<sub>2.5</sub> emission rate and Cycle length, average delay and average stop

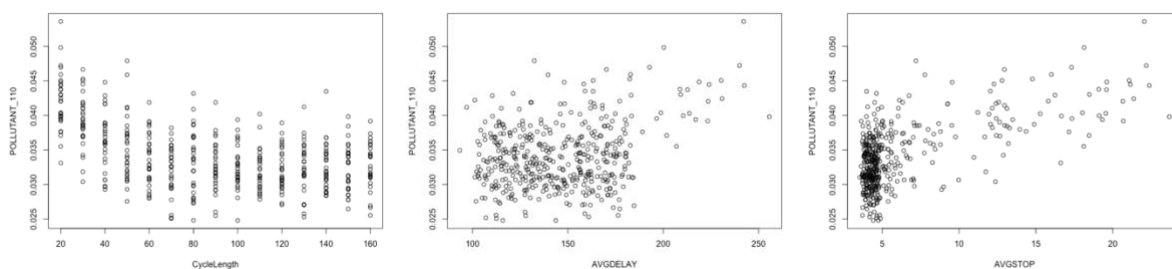


Fig: 35 Plot for PM<sub>2.5</sub> emission with Cycle Length, Average delay, and Average stop

The result for the regression is:

```

Residuals:
      Min       1Q   Median       3Q      Max
-0.0085712 -0.0023986 -0.0003783  0.0023120  0.0123386

Coefficients:
              Estimate Std. Error t value Pr(>|t|)
(Intercept)  2.979e-02  1.004e-03  29.662  <2e-16 ***
CycleLength -5.785e-05  2.882e-05  -2.007  0.0453 *
AVGDELAY     6.452e-05  3.623e-05   1.781  0.0756 .
AVGSTOP     1.890e-05  3.555e-04   0.053  0.9576

---
Signif. codes:  0 '***' 0.001 '**' 0.01 '*' 0.05 '.' 0.1 ' ' 1

Residual standard error: 0.00364 on 446 degrees of freedom
Multiple R-squared:  0.3886,    Adjusted R-squared:  0.3845
F-statistic: 94.51 on 3 and 446 DF,  p-value: < 2.2e-16

```

Fig: 36 Result of Regression for Pollutant 110 (PM2.5)

This regression analysis shows that the relationship between PM2.5 emission rate is statistically significant with cycle length only but not significant with average delay and average stop. Looking at the adjusted R-squared value, which is low, they are not strongly correlated as well.

## 5 Conclusion

The signal timings for an isolated intersection are designed to achieve operational efficiency and safety at the intersection while optimizing the delay. Fig: 6 shows that 70 seconds is an optimal cycle length based on delay, consistent with the optimal cycle length given by the webster's optimal cycle length, which is 67 seconds. Furthermore, this optimal cycle length for delay also does not result in a considerably high stopping rate. From fig: 7, we can see that increasing the cycle length above optimal cycle length does not decrease the stopping significantly; however, decreasing the cycle length below optimal cycle length increases the stopping significantly.

The delay rate and stopping rate impact the vehicle's time in different operating modes (acceleration, cruise, deceleration, and idle). The proportion of time in which a vehicle accelerates decreases with a decrease in the cycle length. The proportion of time in which the vehicle operates in the cruise increases with the cycle length until the webster's optimal cycle length and then remains almost the same. Like acceleration, the proportion of time in deceleration also decreases with the cycle length. Opposite to the cruse, the proportion of the vehicle's time in idle decreases until the optimal cycle length and then starts increasing beyond that.

Different operating modes have different emission rates, and the rates are different for each pollutant. The vehicles in acceleration contribute to the highest proportion of emission for each pollutant. From fig: 23, we can see that, even though the proportion of the vehicle time in acceleration is only 16%, the proportion of emission due to acceleration is more

than 35% for all pollutant types. Furthermore, for each pollutant, the proportion of the emission from acceleration is highest compared to other operating modes, except for HC, in which the cruise has the highest proportion. The highest proportion of emission from acceleration among all pollutants is for CO, which is 60%, which tells that CO emissions occur mainly during acceleration. Another major operation during which there is a high emission is the cruise. However, the proportion of emission from the cruise is almost equal to the proportion of time the vehicles operate under cruise for all the pollutants. Therefore, controlling the proportion of time the vehicle accelerates can help in minimizing the emission.

There are different emission rates for each pollutant for different vehicle types. Moreover, the nature of the curve for the emissions rate with the cycle length is different for different vehicle types. For instance, in CO, the emission rate is decreasing for cars when moving from lower to higher cycle length. In contrast, the emission rate for the bus starts to increase after the cycle length of 80 seconds, and the emission rate for trucks starts to increase after 110 seconds. Due to the different nature of the emission-rate-curve for different vehicle types, each pollutant's emission- rate-curve is the combined effect of the nature of the emission-rates -curve of each vehicle type and the proportion of each vehicle type. Therefore, the nature of the emission rates depends upon the vehicle types and the proportion of each vehicle type. However, the emission rate for each vehicle type is decreasing until the webster's optimal cycle length (70 s) for all of the pollutants, as seen in fig: 14-15. The difference is found only on higher cycle lengths than webster's optimal cycle length among the pollutants. All of this variation resulted in the uneven nature of the

emission rate after the webster's optimal cycle length in each pollutant, as shown in the fig:14.

However, analyzing all the emission trends for all pollutants, we are confident that the range for optimal cycle length for emission rate is equal to or higher than the webster's optimal cycle length. Due to this and the uneven nature of the emission-rate-curve, we cannot decide one optimal cycle length for the emission; therefore, a range is taken. The optimal range for HC, CO, NO<sub>x</sub>, CO<sub>2</sub>, and PM 2.5 is 70s-110s, 100s-120 s, 70s-110s, 70s-120s, and 70s-120s, respectively. The optimal range based on emission considering the maximum overlapping of the ranges between the pollutants is 70 s to 110s.

However, this range of cycle length may not be applicable in all the scenarios. We need to consider the scenarios with different traffic characteristics. If the intersection is in a place where there is a lot of bus services, pedestrians, and bicyclists-- for instance, the downtown area-- we need to prioritize the pedestrians and bike safety to other factors. The range of optimal cycle length would be 70s to 90s because the optimal range of the cycle length for the pedestrians and bike safety is 60s to 90s (NACTO, n.d.). If the intersection is in the industrial areas where there is a high percentage of trucks and no bikes/pedestrians, then the optimal range of cycle lengths would be 90s to 110s. The optimal range is based on the emission-rate-curve of trucks for the pollutants in fig: 14-15, which is decreasing up to the cycle length of 110s for most of the pollutants and even decreasing after that for some pollutants. Finally, if we were to optimize the cycle length for the intersection in the sub-urban area where there are lots of cars and no buses, trucks, and peds/bikes, then 80s to

100s would be the optimal range of cycle length. The optimal range is based on considering NO<sub>x</sub>, PM<sub>2.5</sub>, and CO<sub>2</sub> as important pollution and the nature of emission-rate-curve for these pollutants, shown in fig:14-15.

Finally, the linear regression analysis showed the emission rate is negatively correlated with the cycle length/averaged delay for all pollutants; however, the correlation is only significant (R-squared value greater than 0.8) in CO and CO<sub>2</sub>, even though the relationship is statistically significant (p-value <0.05) for all. Furthermore, adding delay and stopping rates as additional independent variables does not significantly improve the model. Since the emission is negatively correlated with the emission, increasing the cycle length will lower the average emission for the strongly correlated pollutants. For other pollutants, additional quantitative variables should be added to the model.

In this thesis, the recommendation is based on the assumption that the severity of the effect of all emissions is the same. However, this may not be true because different pollutants have different intensities/nature of effects on people's health and the surrounding environment. For instance, reducing 1 gram of PM<sub>2.5</sub> may be more critical than reducing 10 grams of the CO. Since there is a different optimal cycle length for each pollutant, we cannot minimize all the pollutants at once. There is a chance that we may minimize the emission of a less harmful pollutant, resulting in more emission of the harmful pollutant. Therefore, it is necessary to study and categorize the important pollutants and find the amount of one pollutant equivalent to another pollutant in terms of effect. Then the optimal cycle length will reduce the overall effect on the quality of life due to vehicular emission.

Another limitation of this study is that the independent variables in regression on the pollutants is not enough. In the future, regression analysis can be carryout out by adding more independent variables like the Volume-to-Capacity ratio. In this study, the linear model is used for regression; a non-linear model like polynomial, logistic may be more appropriate.

## 6 References

- Abou-Senna, H., Radwin, E., KurtWesterlund, & Cooper, D. C. (2013, April 22). Using a traffic simulation model (VISSIM) with an emissions model (MOVES) to predict emissions from vehicles on a limited-access highway. *Journal of the Air & Waste Management Association*, 63(7). doi:10.1080/10962247.2013.795918
- Braven, K. R., Abdel-Rahim, A., Henrickson, K., & Battles, A. (2012). *MODELING VEHICLE FUEL CONSUMPTION AND EMISSIONS AT SIGNALIZED INTERSECTION APPROACHES: INTEGRATING FIELD-COLLECTED DATA INTO MICROSCOPIC SIMULATION*.
- Chen, K., & Yu, L. (2007). Microscopic Traffic-Emission Simulation and Case Study for Evaluation of Traffic Control Strategies. *J Transpn Sys Eng & IT*, 7(1), 93-100.
- EPA. (2019, September 24). *Light Duty Vehicle Emission*. Retrieved from EPA: <https://www.epa.gov/greenvehicles/light-duty-vehicle-emissions>
- EPA. (2020, July 29). *Fast Facts on Transportation Greenhouse Gas Emissions*. Retrieved from EPA: <https://www.epa.gov/greenvehicles/fast-facts-transportation-greenhouse-gas-emissions>
- EPA. (2020, November 10). *MOVES*. Retrieved from EPA: <https://www.epa.gov/moves#:~:text=EPA's%20MOtor%20Vehicle%20Emission%20Simulator,greenhouse%20gases%2C%20and%20air%20toxics>.
- Giuliano, G., & Hanson, S. (2017). *The Geography of Urban Transportation*. The GUIFORD PRESS.
- ICCT. (2017, October 10). *The International Council on Clean Transportation*. Retrieved from Vehicle NOx emissions: The basics: <https://theicct.org/cards/stack/vehicle-nox-emissions-basics#:~:text=Among%20the%20air%20pollutants%20gasoline,to%20agricultural%20crops%20and%20ecosystems>.
- LeBlanc, D. C., Saunders, F. M., Mayers, M. D., & Guensler, R. (1995). Driving pattern variability and impacts on vehicle carbon monoxide emissions. *TRANSPORTATION RESEARCH RECORD 1472*, TRB, 45-52.
- Li, J.-Q., Wu, G., & Zou, N. (2011, July). Investigation of the impacts of signal timing on vehicle emissions at an isolated intersection. *Transportation Research Part D: Transport and Environment*, 6(5), 409-414;DOI-10.1016/j.trd.2011.03.004.
- Li, X., Li, G., Pang, S.-S., Yang, X., & Tiang, X. (2004). Signal timing of intersections using integrated optimization of traffic quality, emissions and fuel consumption: a note. *Transportation Research Part D: Transport and Environment*, 9(5), 401-407, DOI: 10.1016/j.trd.2004.05.001.
- Mardsen, G., Bell, M., & Reynolds, S. (2001). TOWARDS A REAL-TIME MICROSCOPIC EMISSIONS MODEL. *Transportation Research. Part D: Transport & Environment*, 6(1), 37-60.
- Marsh, B. W. (1949, 04). *Purdue e-pubs*. Retrieved from Purdue Road School: <https://docs.lib.purdue.edu/cgi/viewcontent.cgi?article=2566&context=roadschool>

- NACTO. (n.d.). *Signal Cycle Lengths*. Retrieved from National Association of City Transportation officials: <https://nacto.org/publication/urban-street-design-guide/intersection-design-elements/traffic-signals/signal-cycle-lengths/>
- Rao, Q., Zhang, L., Yang, W., & Fang, B. (2014). Analyze of instantaneous vehicle emission models based on speed and acceleration. *CICTP 2014*, doi:10.1061/9780784413623.262 .
- Ritner, M., Westerlund, K. K., Cooper, C., & Claggett, M. (2013, May). Accounting for acceleration and deceleration emissions in intersection dispersion modeling using MOVES and CAL3QHC. *Journal of the Air & Waste Management Association*, 63(6), 724-736, DOI: 10.1080/10962247.2013.778220 .
- Stevanovic, A., Stevanovic, J., Zhang, K., & Batterman, S. (2009). Optimizing Traffic Control to Reduce Fuel Consumption and Vehicular Emissions. *Transportation Research Record: Journal of the Transportation Research Board*, 2128(1), 105-113:10.3141/2128-11.
- UCS. (2014, July 18). *Vehicles, Air Pollution, and Human Health*. Retrieved from Union of Concerned Scientists: <https://www.ucsusa.org/resources/vehicles-air-pollution-human-health#:~:text=Passenger%20vehicles%20are%20a%20major,hydrocarbons%20emitted%20into%20our%20air.>
- Vanek, F. M., Angenent, L. T., Banks, J. H., Daziano, R. A., & Turnquist, M. A. (2014). *Sustainable Transportation Systems Engineering*. McGraw-Hill Education.
- Wang, Y., Guo, D., Shiwu Li, Wang, Y., & Li, Z. (2009). Signal Timing Optimization Simulation on Urban Road Intersection Based on Vehicle Emissions. *Eighth International Conference of Chinese Logistics and Transportation Professionals*. ASCE.
- Wu, S., Sun, K., & Liu, L. (2020). Urban Traffic Signal Timing Optimization by Reducing Vehicle Emissions. *2020 International Conference on Urban Engineering and Management Science (ICUEMS)* (pp. 361-369, doi: 10.1109/ICUEMS50872.2020.00085.). Zhuhai China: 2020 International Conference on Urban Engineering and Management Science (ICUEMS).
- Zakariya, A. Y., & Rabia, S. I. (2016, August 22). Estimating the minimum delay optimal cycle length based on a time-dependent delay formula. *Alexandria Engineering Journal*, 55(3), 2509-2514.

## Appendix



## Appendix 2: MOVES Vehicle Type and Physics Parameters

MOVES Vehicle Type Name	Vehicle Type ID	Model Years	A	B	C	M	m
Motorcycle	11	1969-2050	0.0251	0	0.000315	0.285	0.285
Passenger Car	21	1969-2050	0.156461	0.002001	0.000492	1.4788	1.4788
Passenger Truck	31	1969-2050	0.22112	0.002837	0.000698	1.86686	1.8668
Light Commercial Truck	32	1969-2050	0.235008	0.003038	0.000747	2.05979	2.0597
Intercity Bus	41	1960-2013	1.29515	0	0.003714	17.1	19.593
		2014-2050	1.23039	0	0.003714	17.1	19.593
Transit Bus	42	1960-2013	1.0944	0	0.003587	17.1	16.556
		2014-2050	1.03968	0	0.003587	17.1	16.556
School Bus	43	1960-2013	0.746718	0	0.002175	17.1	9.0698
		2014-2050	0.709382	0	0.002175	17.1	9.0698
Refuse Truck	51	1960-2013	1.58346	0	0.003572	17.1	23.113
		2014-2050	1.50429	0	0.003572	17.1	23.113
Single-Unit Short Haul Truck	52	1960-2013	0.627922	0	0.001603	17.1	8.5389
		2014-2050	0.596526	0	0.001603	17.1	8.5389
Single-Unit Long Haul Truck	53	1960-2013	0.557262	0	0.001473	17.1	6.9844
		2014-2050	0.529399	0	0.001473	17.1	6.9844
Motor Home	54	1960-2013	0.68987	0	0.002105	17.1	7.5257
		2014-2050	0.655376	0	0.002105	17.1	7.5257
Combination Short Haul Truck	61	1960-2013	1.53819	0	0.004030	17.1	22.974
		2014-2050	1.43052	0	0.003792	17.1	22.828

### Appendix 3: MOVES VSP/STP Operating Mode Bins

Operating Mode ID	Operating Mode Description	Vehicle Specific Power (VSP)	Vehicle Speed	Vehicle Acceleration
		(KW/tonne)	(vt, mph)	(a, mph/sec)
0	Deceleration/Braking			$a_t \leq -2.0$ OR ( $a_t < -1.0$ AND $a_{t-1} < -1.0$ AND $a_{t-2} < -1.0$ )
1	Idle		$-1.0 \leq v_t < 1.0$	Any
11	Coast	$VSP_t < 0$	$0 \leq v_t < 25$	Any
12	Cruise/Acceleration	$0 \leq VSP_t < 3$	$0 \leq v_t < 25$	Any
13	Cruise/Acceleration	$3 \leq VSP_t < 6$	$0 \leq v_t < 25$	Any
14	Cruise/Acceleration	$6 \leq VSP_t < 9$	$0 \leq v_t < 25$	Any
15	Cruise/Acceleration	$9 \leq VSP_t < 12$	$0 \leq v_t < 25$	Any
16	Cruise/Acceleration	$12 \leq VSP_t$	$0 \leq v_t < 25$	Any
21	Coast	$VSP_t < 0$	$25 \leq v_t < 50$	Any
22	Cruise/Acceleration	$0 \leq VSP_t < 3$	$25 \leq v_t < 50$	Any
23	Cruise/Acceleration	$3 \leq VSP_t < 6$	$25 \leq v_t < 50$	Any
24	Cruise/Acceleration	$6 \leq VSP_t < 9$	$25 \leq v_t < 50$	Any

Operating Mode ID	Operating Mode Description	Vehicle Specific Power(VSP)	Vehicle Speed	Vehicle Acceleration
		(KW/tonne)	(vt, mph)	(a, mph/sec)
25	Cruise/Acceleration	$9 \leq VSP_t < 12$	$25 \leq v_t < 50$	Any
27	Cruise/Acceleration	$12 \leq VSP_t < 18$	$25 \leq v_t < 50$	Any
28	Cruise/Acceleration	$18 \leq VSP_t < 24$	$25 \leq v_t < 50$	Any
29	Cruise/Acceleration	$24 \leq VSP_t < 30$	$25 \leq v_t < 50$	Any
30	Cruise/Acceleration	$30 \leq VSP_t$	$25 \leq v_t < 50$	Any
33	Cruise/Acceleration	$VSP_t < 6$	$50 \leq v_t$	Any
35	Cruise/Acceleration	$6 \leq VSP_t < 12$	$50 \leq v_t$	Any
37	Cruise/Acceleration	$12 \leq VSP_t < 18$	$50 \leq v_t$	Any
38	Cruise/Acceleration	$18 \leq VSP_t < 24$	$50 \leq v_t$	Any
39	Cruise/Acceleration	$24 \leq VSP_t < 30$	$50 \leq v_t$	Any
40	Cruise/Acceleration	$30 \leq VSP_t$	$50 \leq v_t$	Any

#### Appendix 4: Age Distribution for year 2020

yearID	ageID	ageFraction21	ageFraction42	ageFraction62
2020	0	0.07044951	0.05768491	0.05121146
2020	1	0.06984896	0.05678244	0.04951647
2020	2	0.06945678	0.0562041	0.04804709
2020	3	0.07038678	0.05406273	0.04518188
2020	4	0.06970372	0.05348556	0.044542
2020	5	0.06749467	0.05107508	0.04252977
2020	6	0.06565985	0.04625069	0.03797247
2020	7	0.0618939	0.0409148	0.03327615
2020	8	0.05876154	0.03700771	0.03151438
2020	9	0.03549266	0.04398609	0.03357943
2020	10	0.03876577	0.02654977	0.02626323
2020	11	0.03417737	0.02655554	0.03421676
2020	12	0.04168821	0.03674548	0.0263633
2020	13	0.0424049	0.03495301	0.09007409
2020	14	0.03504053	0.02473986	0.06590848
2020	15	0.0302467	0.03815712	0.06169877
2020	16	0.02412173	0.03075893	0.03633657
2020	17	0.02133138	0.02963533	0.03501233
2020	18	0.01788057	0.02940897	0.02508641
2020	19	0.01450821	0.03323322	0.02840009
2020	20	0.01310978	0.02200854	0.04450793
2020	21	0.00962224	0.02097952	0.03249449
2020	22	0.00736834	0.02421211	0.0213483
2020	23	0.00639744	0.02169105	0.01189218

yearID	ageID	ageFraction21	ageFraction42	ageFraction62
2020	24	0.00501109	0.01963849	0.01267178
2020	25	0.00491689	0.01587882	0.01119392
2020	26	0.0037155	0.01357604	0.00661354
2020	27	0.00309115	0.01110526	0.00442687
2020	28	0.00252931	0.00953515	0.00261892
2020	29	0.00210301	0.00945485	0.00197812
2020	30	0.00282153	0.02373085	0.00352265